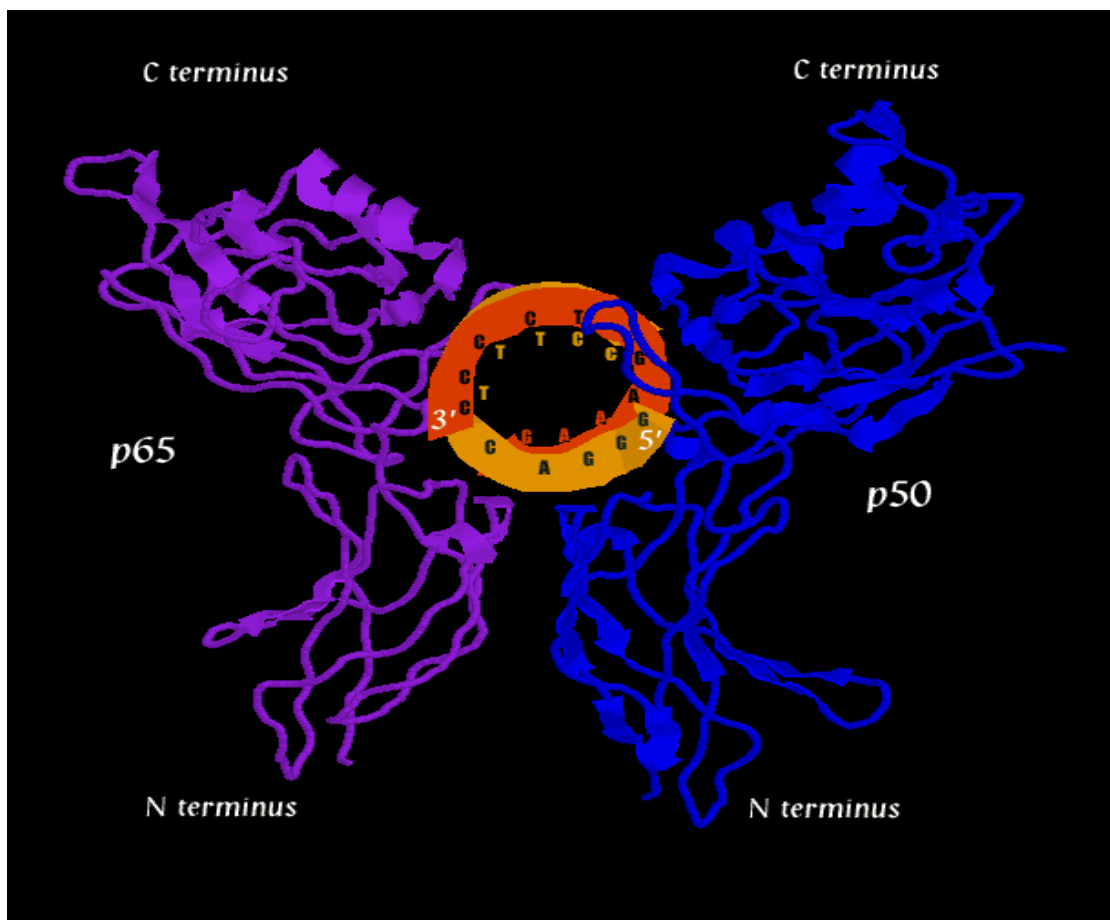




MOLECULAR BASIS
OF HUMAN DISEASES
ΚΥΤΤΑΡΙΚΗ ΚΑΙ ΓΕΝΕΤΙΚΗ ΑΙΤΙΟΛΟΓΙΑ
ΔΙΑΓΝΩΣΤΙΚΗ ΚΑΙ ΘΕΡΑΠΕΥΤΙΚΗ
ΤΩΝ ΑΣΘΕΝΕΙΩΝ ΤΟΥ ΑΝΘΡΩΠΟΥ

Transcriptional Regulation of murine IRAK-M

by Liapis Ioannis



Supervisor: Dr. Christos Tsatsanis

List of contents

Summary	3
A. Introduction	5
A1. A brief historical overview	5
A2. IRAK-M gene and protein	6
A3. Function of IRAK-M	7
A4. Evidence linking IRAK-M to TLR induced tolerance	8
A5. Tolerance outside TLR and cytokine signaling	9
A6. IRAK-M regulation	10
A7. Aims	11
B. Materials and Methods.	12
B1. Cloning and Constructs	12
B2. Transfections	13
B3. RNA extraction and quantification	14
B4. Chromatin immunoprecipitation	15
C. Results	
A. Online data mining and in silico analysis	18
A1. Data available in public online databases	18
A2. In silico analysis of the sequence upstream of irak3	20
B. Experimental assays	21
B1. Upstream sequences of irak3 respond to LPS stimulation	21
B2. IFN- α 3 and IL-10 do not upregulate IRAK-M	22
B3. Binding of NF- κ B in predicted sites of IRAK-M promoter	24
B4. LPS induced binding of C/EBP β	25
D. Discussion	27
E. Future Prospects	28
Z. References	29

Summary

Innate immune responses are imperative for the successful defense against endogenous and exogenous threats. However, excess activation can have adverse repercussions and ultimately lead to autoimmune phenomena and irreparable tissue damage. Thus, innate mediators such as monocytes/macrophages have developed a complex system of self regulation that essentially leads to a tolerant and anti-inflammatory phenotype. Among the mechanisms that govern this phenomenon, is the upregulation of molecules that limit signaling downstream of the TLR4 receptor, which recognizes LPS as its ligand.

IRAK-M was first identified in 1999 as a member of the irak family of serine / threonine kinases which enable signal transduction downstream of many TLRs and IL-1 β . Originally thought to play a redundant part in this process, it was later shown that in fact is an inactive member, with a non functioning kinase domain. Moreover, ever since 2002 it is considered as one of most important negative regulators of the TLR signaling pathway: primary macrophages from IRAK-M deficient mice, exhibit an intrinsic inability to become tolerant after prolonged LPS stimulation and upon challenging, they are characterized by a profile of increased pro-inflammatory cytokine expression and excess activation of mediators downstream of the TLR signaling complex. In more recent publications, IRAK-M is constantly found upregulated under tolerogenic conditions, in a process that is time and stimulus strength dependent: within boundaries, higher concentrations of TLR ligands and longer incubation periods confer increased IRAK-M mRNA levels. Lastly the role of IRAK-M in regulating innate immunity activation is validated by numerous epidemiological and clinical data.

Despite the relatively good understanding of its mechanism of function, too few are actually known about the actual transcriptional regulation of the IRAK-M gene: many publications exhibit IRAK-M upregulation upon stimulation with a diversity of TLR ligands, however the molecular mechanisms governing this process are still well hidden. Information about transcription factors and signaling pathways that govern its expression is scarce, scattered and fragmented. Roles for PU.1, glucocorticosteroid receptor and SMAD 4 have been suggested but all the evidence is indirect. Also, adiponectin, an adipocyte secreted hormone is able to regulate IRAK-M expression via PI3K/akt and tpl2/ERK dependent mechanisms. Lastly of particular interest are recent publications revealing additional levels in IRAK-M regulation: cellular compartmentalization and trafficking.

The aim of this study is essentially to help in elucidating the mechanisms governing IRAK-M's expression at the core transcriptional level. We aim to identify key transcription factors that enable this process and decipher their own regulation in the context of inflammation and immune tolerance, events that are timely and functionally discriminated. Lastly it should be noted that this work is a continuation of our efforts in identifying the mechanisms governing PI3K/akt induced tolerance in cells of the innate immunity.

Online data mining revealed that the transcription start site of IRAK-M should be located at a region approximately 90 to 100 base pairs upstream of its translation site (1st exon). This correlates well with cross species homology observations. Moreover, in silico analysis of non coding sequences upstream of the IRAK-M gene revealed that IRAK-M is a TATA-less gene

and significant clustering of relevant transcription factor binding sites proximally to the putative transcription start region.

We dissected upstream non coding sequences and have found that LPS is able to transduce IRAK-M expression through an NF- κ B binding site, located approximately 339 base pairs upstream of the translation start site. NF- κ B, a key mediator of intracellular LPS signaling, is able to bind directly on this site upon short term LPS stimulation in RAW 264.7 mouse macrophages and transactivate the IRAK-M gene. Moreover we show that IFN- α and IL-10 are unable to upregulate IRAK-M and theorize on putative suppressive effects via direct NF- κ B-STAT competition on IRAK-M promoter.

Also, we provide further evidence that PI3K/akt signaling affects IRAK-M transcription, as previously stated, by exhibiting interplay with C/EBP β , an important transcription factor induced upon inflammatory stimuli. LPS is able to promote physical C/EBP β binding on IRAK-M promoter, in a process largely dependent on PI3K/akt signaling, as treatment with wortmanin –a PI3K inhibitor is able to abrogate this phenomenon.

Thus, these data point towards an old and basic theme in immunobiology: Signaling pathways essentially lead their own inactivation. Here we show that TLR4 signaling promotes its inactivation, by utilizing two of the transcription factors that confer its inflammatory effect.

A. Introduction

Immune responses are imperative for the protection of an organism against exogenous or endogenous threats, such as pathogens and cancer respectively. Vertebrates have developed a complicated recognition system in order to effectively guard themselves, which involves both fast acting innate and slowly activated adaptive immune responses. In the case of the former, innate immune cells such as monocytes/macrophages are able to detect stereotypic molecules through their pattern recognition receptors (PRRs) and thus trigger the initiation events of inflammation [1]. A receptor of this kind, TLR4, is known to bind LPS (Lipopolysaccharide, Endotoxin) –a native component of Gram (-) bacteria's cell wall[1,2].

Whereas sustained inflammation is imperative to battling pathogens, excessive inflammation on the other hand can lead to irreparable tissue damage. Thus, immune responses, physiologically, are tightly regulated and in many cases self-restricted via negative feedback signaling loops. For example, in the case of TLR4, persistent stimulation with endotoxin renders responsive cells into a transient anergic and tolerant state, under which restimulation with LPS is unable to transduce the early pro-inflammatory features, a phenomenon termed Endotoxin Tolerance [3]. This altered status is believed to be the net result of an accordingly altered transcriptional profile. Thus, tolerant macrophages are characterized by the down-regulation of pro-inflammatory cytokines, the up-regulation of anti-inflammatory cytokines (and cytokine antagonists such as IL-1Ra) and decreased antigen presentation capability, as conferred by the down-regulation of MHC-II molecules and CIITA [4].

Since the stimulus required for the induction of the tolerant status is an inflammatory one (in the case of endotoxin tolerance LPS itself), it is only natural that this phenomenon works in negative feedback loops: activation of TLR signaling pathways leads essentially to their own dampening. This involves either the downregulation of key effector molecules in the TLR signaling pathway, such as the TLR4 receptor[5], or the upregulation of negative regulators such as SOCS-1 [6], A20[7] and IRAK-M[8]. Regulation is performed at a post transcriptional level also, with the modulation of miRNA expression [9].

Ever since 2002, IRAK-M is firmly linked with endotoxin tolerance. This study focuses exclusively on IRAK-M and its transcriptional regulation in the initiating events that confer tolerance to LPS.

A1. A brief historical overview

Screening of ESTs for sequences sharing significant homology with the human Irak gene led to the discovery of Irak-m in 1999. Wesche et al [10] were able to clone the cDNA encoding for this novel protein and classify it as a member of the Irak family of kinases which serve as intracellular signal transducers of various pro-inflammatory stimuli such as LPS or IL-1. The name IRAK-M was appointed because of the restriction in this molecule's expression in cells of monocytic origin. Moreover, functional ex vivo proteomic characterization placed Irak-m firmly in the IRAK signaling cascade and led Wesche et al to propose that it could serve a redundant role in a pathway predominantly occupied by IRAK-1.

The discovery of the murine counterpart to human Irak-m was reported in 2002 by two distinct publications. The first one, by Rosati and Martin [11], identified murine Irak-m as a

68kDa protein of 609 amino acids, sharing 71% homology with human Irak-M and displaying the same pattern of minimal autophosphorylation activity in *in vitro* assays. The second one, by Kobayashi et al [8] is probably the most influential publication on this protein's fate. It is the first publication to ever attribute an inhibitory -rather than an effector role for IRAK-M in proinflammatory signal transduction and to stably associate it with the induction of endotoxin tolerance in murine macrophages. Moreover it is the first publication to report the generation of IRAK-M knockout mice.

Ever since 2002 IRAK-M is considered as one of the most important inducers of macrophage tolerance. Its role in attenuating TLR signaling in innate immunity has been elucidated by utilizing both *ex vivo* and *in vitro* studies and research performed in IRAK-M knock out animals. Moreover, newer data provide further insight in its cellular distribution and function, while linking it with adaptive immune responses too. Additionally, beside the hard molecular data, the truth in this primary function is strengthened even further by rapidly accumulating evidence from epidemiological studies associating IRAK-M with human disease.

A2.IRAK-M gene and protein

The human *irak3* gene is mapped at chromosome 12 (12q14.3, negative strand) spanning over 65 kb. It is comprised of 12 exons. An alternative splice variant of 11 exons (skipping the second exon) of unknown functionality also exists. Northern blot analysis has shown that IRAK-M is expressed predominantly in peripheral blood leukocytes. It is also expressed in the U937 and THP1 cell lines [10]. Polarization of the THP1 cell line towards macrophages further increases its expression. Human *irak-m* gene encodes for a 68kDa protein of 596 amino acids. The protein shares a 30- 40% homology with other members of the IRAK family of kinases [10]. *In vitro* proteomic analysis has shown that human IRAK-M can be precipitated along with Traf6, MyD88 and members of the IRAK family [10].

Murine IRAK-M is mapped in chromosome 10, spans over 60 kb and is comprised of 12 exons. Northern blot analysis revealed that murine *irak-m* is expressed in all murine tissues and most predominantly in the liver and thymus. It is also expressed in NIH3T3 fibroblasts and RAW 364.7 mouse macrophages[11].It encodes for a 68.7kDa protein of 593 amino acids sharing a 73% homology with murine IRAK1[8].

Both human and murine IRAK-M exhibit proteomic characteristics of the IRAK family: an amino terminal death domain (DD), a central kinase domain and a carboxy terminal stretch [10,12]. The DD was recently shown to facilitate the interaction with IRAK-1[38]. Truncated IRAK1 for its carboxy-terminal domain retains its ability to bind IRAK-M[38]. The kinase domain can be subdivided into 12 serine/threonine subdomains. Whereas IRAK-M contains a functional ATP binding pocket in subdomain II, the kinase catalytic domain in subdomain IVB is inactive[8,10,12]. Namely a critical aspartate residue is replaced by a serine residue. Thus both murine and human IRAK-M have weak autophosphorylation activity[10]. The carboxy terminal stretch can be divided into two functional subdomains: C1 and C2. In the case of IRAK-1, it has been shown that each subdomain confers the ability for TRAF6 association via the conserved Pro-X-Glu-X-X-(aromatic/acidic residue) motif [13].Such motifs are not present in IRAK-M.

A3.Function

Members of the Irak family of kinases are thought to regulate signal transduction from several TLRs and cytokine receptors such as IL-1. In brief, these receptors do not possess intrinsic kinase activity. Instead, upon ligand engagement through their LRR (Leucine rich repeats) extracellular domains, they are able to attract intracellular adaptor molecules such as MyD88. MyD88 in particular, has two domains used for protein to protein interactions: a TIR domain for binding onto the respective TIR domain of the TLR and a death domain (DD), which facilitates interactions with downstream molecules carrying similar death domains [1]. All the members of the Irak family of kinases carry such motifs. Irak1 and Irak4 have been shown to physically interact with MyD88 [14]. This interaction in the receptor complex leads to their auto or cross phosphorylation. Phosphorylated Irak-1 and Irak-4 demonstrate reduced affinity for MyD88 but increased affinity for Traf6[14,15]. Thus they escape the receptor complex and form a heterodimer that is able to interact with Tak1 at the cell membrane. Tak1 along with TAB1, TAB2 and TRAF6 are released together into the cytosol without the participation of IRAK and form an active kinase complex with the participation of other proteins [16]. IRAK-1, remains in the cell membrane and is subsequently ubiquitinated and targeted for proteosomal degradation [16].

The most notable substrates of the TAK1/TRAF6/TAB1/TAB2 complex include IKKa/b leading to the activation of the canonical NF- κ B pathway, MAP2K3/4/6 phosphorylation also leading to NF- κ B induction, MAPK p38 which regulates ATF and Ets mediated transcription (among others) and JNK which leads to AP1 coupled transcription[17].

It has to be noted that IRAK-4 is considered to be more important than IRAK-1 in the activation of the canonical NF- κ B pathway: whereas IRAK-4 knockout mice exhibit a severe impairment in TLR induced NF- κ B activation[18], IRAK-1 knockouts exhibit a less severe impairment coupled with unchanged I κ B α degradation[19]. However IRAK-1 can promote p65/RelA phosphorylation and has been shown to facilitate STAT and IRF5/7 phosphorylation[20]. A more detailed description of the IRAK-mediated TLR signaling pathways can be found in these reviews [12, 21].

As previously mentioned, IRAK-M is one of the major negative regulators of this pathway. Being a member of the IRAK family it has all the structural characteristics of the other members, albeit a minimally active kinase catalytical centre [8, 10]. Also proteomic analysis has shown that human IRAK-m can be precipitated along with MyD88, TRAF6 and other family members of the Irak family in transiently transfected HEK cells [10]. IRAK-M can also physically interact with TIRP, another adaptor protein containing a TIR domain [37]. Additionally murine IRAK-M is able to inhibit IRAK phosphorylation but at the same time increase the ratio of phosphorylated IRAK bound to MyD88, despite the reduction in the affinity between these two molecules following IRAK phosphorylation[8]. Thus, placement of this molecule in the TLR/IL-1 signaling cascades should be dictated by these characteristics.

Kobayashi et al [8] proposed two hypothetical mechanisms that could explain these data: IRAK-M negatively regulates intracellular TLR signaling by either antagonizing for effector IRAK phosphorylation, or by stabilizing the TLR4/MyD88/IRAK1-4 complex [8]. Thus functioning as a physiological dominant negative member of the IRAK family, IRAK-M inhibits the TLR signaling pathway, at an early stage. If this is true and IRAK-M should be able to inhibit this pathway at its early transduction stages, then a complete attenuation of branches is expected. Accordingly, bone derived macrophages from IRAK-M knockout mice upon CpG

or LPS stimulation, exhibit increased phosphorylation of I κ B α , JNK, p38 and ERK1/2[8]. However discrepancies in this theory do exist:

Wesche et al demonstrated that transient transfection of IRAK-M in IRAK-1 deficient HEK 293 cells is able to reconstitute NF- κ B activation [10].

Su et al [22] demonstrated that Pam3CSK4 (a TLR2 agonist)-stimulated, IRAK-M deficient macrophages exhibit increased phosphorylation of p38 MAPK, but not of ERK or JNK. IRAK-M is shown in THP1 cells to exert attenuation p38 activation through decreasing proteosomal degradation of MKP1, a known inhibitor of p38 MAPK.

Pam3CSK4, has also been shown to preferentially activate the alternative NF- κ B signaling pathway [23]. In IRAK-M $-/-$ macrophages, cellular fragmentation assays revealed that Pam3CSK4 favors RelB instead of RelA nuclear translocation. Moreover, NIK stability is increased in IRAK-M deficient macrophages, as is the ratio of IKK α /IKK β homodimers[23]. Discrepancies related to Pam3CSK4 could suggest that IRAK-M function is ligand/receptor specific.

A4.Evidence linking IRAK-M to TLR induced tolerance

Probably the most convincing piece of evidence linking IRAK-M to TLR induced tolerance in innate immunity is observations done in IRAK-M knockout mice. They were first generated by Kobayashi et al in 2002[8]. These animals appear normal in their gross anatomy, but distinctly display a pro-inflammatory phenotype: Primary macrophages from these animals have an intrinsic inability to become tolerant up until a 24 hour stimulation with TLR agonists: upon challenging with various TLR ligands (or IL-1) or infection with Gram (+) or Gram(-) bacteria, IRAK-M deficient macrophages produce reduced levels of IL-12p40, IL-6 and TNF α . Accordingly, upon TLR stimulation, they also exhibit a substantial increase in cytokine secretion and activation of effector molecules downstream of TLR signaling, such as NF- κ B, JNK, p38 and ERK1/2[8]. IRAK-M $-/-$ mice infected orally with *Salmonella typhimurium*, develop more severe enteritis and an increase of both the size and the number of Peyer's patches when compared to wild type counterparts [8]. Eventually, these animals develop severe osteoporosis, evident in just 4 months after birth due to a substantial increase in the osteoclast number [24]. As shown in ex vivo cell cultures this increase is the net result of accelerated osteoclast differentiation and increased osteoclast survival. Moreover IRAK-M $-/-$ osteoclasts also exhibit a similar intrinsic pro-inflammatory phenotype to their IRAK-M $-/-$ monocytic progenitors: both IL-1 and LPS stimulation hyperactivate the canonical NF- κ B pathway and MAPK signaling [24].

IRAK-M deficient mice exhibit higher survival rates when competing in an experimental model for sepsis[30]. Knocking down IRAK-M has also been shown to confer similar effects: SiRNA inhibition of IRAK-M is able to reconstitute the secretion of proinflammatory cytokines in otherwise TLR-tolerant macrophages[25,29,32].

Another indication is the common observation of increased IRAK-M mRNA and protein levels upon TLR ligand stimulation. A list of known inducers of IRAK-M expression can be found in **Table 1**. Whereas, a basal level of IRAK-M expression is present in unstimulated human and murine monocytes/macrophages[8,10,36], transcription of IRAK-M is exponentially induced shortly after TLR ligand stimulation and progresses in fashion analogous to stimulus strength: higher concentrations of TLR ligands and longer incubation periods confer increased IRAK-M mRNA levels[4,8,35,36]. In all listed publications, increased IRAK-M mRNA and protein levels

effectively correlate with the consolidation of tolerance in effector cells of innate immunity. These characteristics of IRAK-M expression have been validated in murine and human models for sepsis [30,39].

Table 1: a list of all molecules shown to upregulate IRAK-M

Molecule	Receptor	Background
LPS	TLR4	Bone marrow derived mouse macrophages[8][31] Peripheral blood human monocytes[26]
Peptidoglycan (30 µg/ml)	TLR2	RAW 264.7 mouse macrophages[25]
Hyaluronan	TLR4, CD44	Peripheral blood human monocytes[28]
Mannose-capped lipoarabinomannan	TLR2 MannoseR	RAW 264.7 mouse macrophages[29]
Pam3CSK4	TLR1/2	Peripheral blood human monocytes[22],[34],[35]
SM360320	TLR7	Bone marrow derived mouse macrophages[33]
Imiquimod R837	TLR7	RAW 264.7 mouse macrophages[34]
IL-1a	IL-1R	Bone marrow derived mouse macrophages[24]
TNFa	TNFR	Peripheral blood human monocytes[27]
MDP	Nod2	Peripheral blood human monocytes[32]
RANKL	RANK	Ex vivo RANKL-differentiated osteoclasts[24]
Adiponectin (gAd)	AdipoR1 AdipoR2	Thioglycolate-elicited mouse macrophages[36]

A5.Tolerance outside TLR and cytokine signaling

Tolerance in innate immunity is a phenomenon not strictly restricted to TLR stimulation but involves other facets of human disease such as cancer. Human monocytes co-cultured in the presence of various cancer cell lines display a tolerant phenotype and high levels of IRAK-M expression [28]. Hyaluronan, a glycosaminoglycan secreted by tumor cells is able to promote tolerance and IRAK-M expression via CD44 and TLR4 mediated mechanisms[28]. IRAK-M deficient mice are resistant to tumor growth upon transplantation of tumor cells[50]. This property correlates with an increase in T effector cells, a decrease in Treg population, increased lymphocyte proliferation and potent macrophage activation [50].

Collectively it is clear that IRAK-M has potent immunomodulatory properties and is able to promote tolerance under various circumstances. Moreover, this ability correlates with numerous clinical and epidemiological data: monocytes derived from 5 patients suffering from moderate sepsis, upon restimulation with LPS exhibited a tolerant phenotype coupled with significant IRAK-M upregulation [25]. Monocytes from patients suffering from chronic myeloid leukemia exhibit high levels of IRAK-M expression [28]. Monocytes from 30 children suffering from Multi Organ Dysfunction Syndrome (MODS) exhibited increased levels of IRAK-M mRNA [40]. Similar observations were made in a study of 34 ACS (Acute Coronary Syndrome) patients [41]. High IRAK-M levels were shown to correlate with mortality in Gram

(-) sepsis[42]. Lastly, mutations in coding sections of the *irak3* gene have been linked with early onset persistent asthma in Italian populations [43].

A6.IRAK-M regulation

Despite the firm association of IRAK-M to endotoxin tolerance and the relative good understanding of its mechanism of function, too few are known about the actual transcriptional regulation of this gene: whereas cytokines (such as IL1[24], and TNF α [27]) and many TLR ligands -such as LPS (TLR4 agonist) [8], hyaluronan [28]and Pam3CSK4 [34] (TLR2 agonists), have all been shown to promote IRAK-M expression, the mechanisms enabling these inductions are still well hidden. IRAK-M promoter is not yet characterized and no firm association between specialized transcription factors and IRAK-M expression exists. For example PU.1 has been shown to promote IRAK-M transcription: IRAK-M is not transcribed in the mAM (mouse Alveolar Macrophage cell line derived from GM-CSF deficient animals), in which PU.1 coupled transcription is not present. Adenoviral reconstitution of PU.1 salvages IRAK-M transcription [44]. However PU.1 responsive sequences in the IRAK-M promoter are not characterized and direct binding of PU.1 is not exhibited.

The elucidation of the molecular pathways that enable IRAK-M transcription could help in identifying putative key transcription factors. Since the main stimulus for IRAK-M induction is signaling through the TLR cascade of events, transcription factors that are activated by this process should have an impact in IRAK-M transcription. In this way TLR stimulation is self restricted and IRAK-M could help in forming a negative feedback loop that inhibits excess monocyte/macrophage activation. Moreover, other molecules with immunomodulatory properties such as hormones or growth factors could also have an effect in IRAK-M transcription. In this sense, 6-Methylprednisone (6-MP) is able to suppress IRAK-M transcription in in vitro differentiated osteoclasts [45]. 6-MP incubated osteoclasts exhibit an activated phenotype coupled with ERK activation [45].

On the other hand, globular adiponectin (gAd), has been shown to increase IRAK-M expression and promote tolerance in mouse macrophages [36]. gAd however cannot repeat this phenomenon in the presence of MEK and/or Akt1 inhibitors (UO126 and wortmannin respectively) or in in the background of akt1 and tpl2 deficient mouse macrophages. Thus, adiponectin could upregulate IRAK-M transcription through Akt1 and tpl2-ERK1/2 mediated processes [36]. These two signaling pathways have been repeatedly shown to regulate transcription factors involved in inflammatory processes. Lastly, despite the lack in experimental data, a role for TGF- β signaling and other anti-inflammatory cytokines in IRAK-M induction should not be excluded. TGF- β has been shown to induce endotoxin tolerance [46]. Since tolerant macrophages do secrete TGF β , paracrine or autocrine mechanisms could be involved in IRAK-M upregulation upon tolerance. Moreover, a recent report attributes to SMAD4 a direct effect in IRAK-M transcription [58].

Synthetic gangliosides GM1 and GD1a have also been shown to inhibit TLR signaling and promote rapid and reversible tolerance in human peripheral blood monocytes. While the mechanisms governing this phenomenon are largely unknown, enrichment of cell membrane with gangliosides is reported to upregulate IRAK-M [47].

Lastly recent reports attribute another level to IRAK-M regulation: cell trafficking and compartmentalization. In the enterocytes TLR signaling takes places in the Golgi apparatus[48].In an experimental model of necrotic enterocolitis, TLR9 signaling is shown to

attenuate the pro-inflammatory, pro-apoptotic TLR4 signaling, thus exerting an anti-inflammatory and protective effect in the intestinal epithelial[49]. In in vitro cultured IEC-6 cells this phenomenon is exerted via IRAK-M. In just 30 minutes upon CpG (TLR9 ligand) stimulation, IRAK-M displays increased co-localization with TLR4 in the Golgi apparatus, whereas co-localization of IRAK-1 and TRAF6 is severely reduced. Moreover knocking down IRAK-M reinstates proinflammatory features observed upon TLR4 signaling. Importantly CpG induction to IRAK-M, cannot be attributed to transcriptional activation since this phenomenon has rapid kinetics. Thus TLR9 signaling in intestinal epithelia could facilitate the redistribution of pre-formed IRAK-M [49].

Utilizing cell fragmentation assays in THP1 cells and in situ immunofluorescence in murine bone marrow derived macrophages, Su et al [22] illustrated that IRAK-M distribution involves both the cytoplasmic and the nuclear compartment. Upon Pam3CSK4 stimulation, IRAK-M becomes exclusively cytoplasmic whereas incubation with leptomycin, a nuclear export inhibitor retains it inside the nucleus. The biological significance of this finding requires further clarification.

A7.Aims

As previously stated, knowledge on IRAK-M transcriptional regulation is scarce, scattered and fragmented. This study aspires to help in elucidating the mechanisms governing IRAK-M's expression at the core transcriptional level. We aim to identify key transcription factors that enable this process and decipher their own regulation in the context of inflammation and immune tolerance, events that are timely and functionally discriminated. Lastly it should be noted that this work is a continuation of our efforts in identifying the mechanisms governing PI3K/akt induced tolerance in cells of the innate immunity.

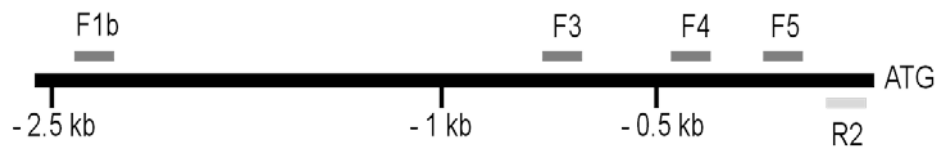
B. Materials and Methods.

1. Cloning and Constructs

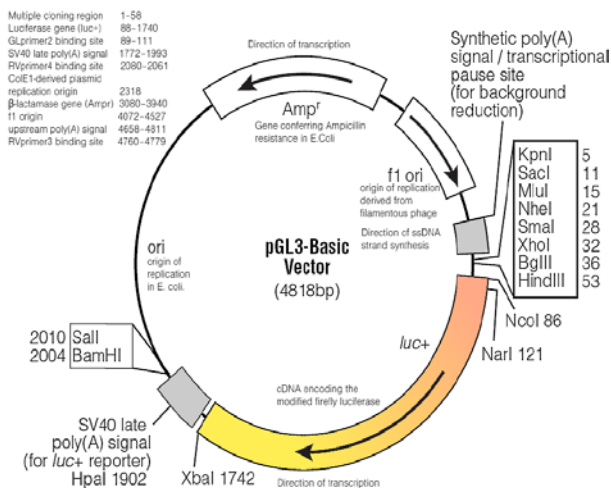
Mouse genomic DNA was used to amplify sequences upstream of mouse *irak3* promoter via PCR. 4 such sequences were created, utilizing a common synthetic reverse primer with a BglIII restriction site and 4 different forward primers, all containing a SacI restriction site. Corresponding primers generating different lengths of genomic sequences are noted in **box 1** and visualized in picture 1.

Box 1

Primer name	Sequence	PCR product length (Fx/R2)
F1	5' AGC CGA GCT CTG AGG AGA ACC GTT TGA GG 3'	2356 bp
F3	5' ACC GAG CTG TTT TCC CAC CTC CTT TGT CAG 3'	746 bp
F4	5' ACC GAG CTC CCT GAC GGG ACA AAG 3'	445 bp
F5	5' ACC GAG CTC GCG GCT AGG AGC AAG 3'	120 bp
R2	5' TTA CTC GAC AGA GAA GCA GGG AGG TC 3'	



Four 45-cycle PCR reactions for each primer pair were carried out. Products were purified via the Qiagen QIAquick Purification Kit according to manufacturer's instructions and resuspended with elution buffer in a final volume of 15µl. All four generated sequences were cut separately via SacI and BglIII, both supplied by Minotech Biotechnology in 3 hour long double digestions, according to manufacturers' instructions.



5 µg of the Promega pGL3basic vector (Cat No E1751) (**Picture 1**) was also digested, as described for the PCR products. Upon digestion, vector 5' dephosphorylation was performed, utilizing 10 units of NEB Antarctic Phosphatase, according to manufacturer's instructions.

Picture 1: The pGL3basic vector

For the ligation reaction an insert/vector=3/1 molar ratio was selected. Depending on insert size, the corresponding amount of digested insert was mixed with 17 ng of digested and dephosphorylated vector (**Box 2**). Relative amounts are shown in box 2. Ligation reactions (of 20µl), utilizing T4 ligase and ATP (Minotech Biotechnology), were performed according to manufacturer's instructions at 16°C overnight.

	Insert
F1	24,4ng
F3	8ng
F4	4,7ng
F5	1,6ng

Box 2

Recombined plasmids were inserted into competent DH10B E. coli via heat shock as follows: 100µl of frozen competent bacteria were thawed on ice and mixed with 10 µl of the ligation product. The mixture was left on ice for 45 minutes and then incubated at 42°C for one minute. After the one minute incubation, the mixture was returned on ice for another five minutes. 800µl of L-broth medium was added and the transformed bacteria were incubated in the hot room for 1 hour, before being plated on L-agar plates with ampicillin. Plates were incubated at 37°C overnight. The following morning colonies were transferred into 3 ml L-Broth with ampicillin under sterile conditions. Liquid bacterial cultures were again incubated at 37°C overnight, under constant stirring.

On the following day, 1 ml of the liquid bacterial cultures was centrifuged at 12000 rpm for 1 minute, to create a bacterial pellet. Supernatant was discarded and the bacterial pellets were resuspended in 100µl of **Solution I**. Then 200 µl of **Solution II** was added and the samples were mixed by inverting 6 times. After 5 minutes on ice, 150µl of ice cold **Solution III** was added, samples were vortexed and returned on ice for another 5 minutes. Samples were then centrifuged at 12000 rpm for 5 minutes. Supernatant was retrieved and subjected to PCI nucleic acid extraction and ethanol precipitation.

Solution I (resuspension): 25mM Tris-HCl (pH 8.0), 10mM EDTA, 50mM Glucose

Solution II (lysis): 200mM NaOH, 1% SDS

Solution III (neutralization): 5M CH₃COONa, glacial acetic acid

Colonies bearing successfully recombined plasmids were verified via 2 double digestions, one utilizing the restriction enzymes for the recombination site (SacI and BglII) and one utilizing enzymes (XbaI and SacII) cutting both the vector and sequences inside the insert to generate linear fragments. Upon verification, 70% bacterial - glycerol stocks were prepared from positive colonies and frozen at -80°C. Plasmid amplification via midi preparation was performed via inoculation of 200 ml L-Broth liquid medium (with ampicillin) with 10µl of 70% glycerol stock, using the Invitrogen PureLink™ HiPure Plasmid Purification Kit, according to manufacturer's instructions.

2. Transfections:

Method of choice was electroporation. 2.5 million RAW 264.7 mouse macrophages grown in DMEM with 10% FBS, 100 U/ml penicillin, and 0.1 mg/ml streptomycin were used per transfection. Assays were performed in either triplets or doublets per variable. 6 µg of recombined plasmid DNA was used in each transfection. Protocol was carried out as follows: Upon counting, the needed number of RAW 264.7 mouse macrophages, already sustained in DMEM with 10% FBS, 100 U/ml penicillin, and 0.1 mg/ml streptomycin, was spanned down by centrifuge at 1500rpm for 5 minutes in 50ml falcons. DMEM was emptied and the cells were resuspended in corresponding volumes of hypo-osmolar electroporation buffer (Eppendorf, Cat no 4308 070.501), producing the needed concentration of 3,125 million cells per ml (or 2,5 million per 800µl). The total volume was further divided in 7 fractions contained in 50 ml falcons, each corresponding to the 6 different plasmids used (F1, F3, F4, F5, Fm, vector) plus mock transfection (no plasmid used) and the correct amount of plasmid (6µg per transfection) was added directly into each fraction and mixed. The Renilla-luciferase vector (Dual-Luciferase® Reporter Assay System Cat No E1910) was added (3µg per transfection) in the same fashion in indicated experiments. Falcons were then kept in ice until electroporation was carried out.

For the electroporation assay 800µl from each plasmid (or mock) enriched fraction were transferred into a 4mm cuvette. The latter was then pulsed with 570 mV, three times in the timecourse of 2 minutes. Transfected cells were left inside the cuvette, in room temperature for 10 minutes and then transferred into a well of a 12-well plate filled with 3ml of DMEM (10% FBS, 100 U/ml penicillin, and 0.1 mg/ml streptomycin). After two hours of incubation at 37°C, the cells were collected again and spanned down (via centrifuge at 1500 rpm for 5 minutes). The pellet of transfected cells was resuspended into 1ml of new DMEM (10% FBS, 100 U/ml penicillin, and 0.1 mg/ml streptomycin) and transferred again unto the same well. Transfected cells were rested at 37°C for approximately 7-10 hours. Subsequently they were starved in DMEM (1% penstrep, no FBS) and simultaneously subjected into a 24 hour long incubation at 37°C in the presence of either 1µg/ml LPS (purchased from Sigma-Aldrich), 10ng/ml recombinated mouse IL-10 (eBioscience Cat No 14-8101), 100IU/ml recombinated mouse IFN-α3 (PBL Interferon source Cat no 12100-1) or none. A 24 hour long stimulation period was selected for sufficient firefly luciferase accumulation, whereas starvation was sufficient in reducing assay background.

Upon endpoint, wells were emptied of culture medium and washed with ice-cold PBS. 100µl of 1X Promega Passive Lysis Buffer (Cat No E1941) was added in each well and plates were shaken for 15 minutes in room temperature. Lysates were collected and centrifuged at 5000rpm, 4°C for 15 minutes. Supernatants were collected and luciferase activity (firefly or Renilla) in each sample was measured using the Promega Dual-Luciferase[®] Reporter Assay System (Cat No E1910) according to manufacturer's instructions.

3. RNA extraction and quantification

500.000 per sample RAW 264.7 mouse macrophages were plated in 12 well plates containing 1 ml DMEM (10% FBS, 100 U/ml penicillin, and 0.1 mg/ml streptomycin). After 16-24 hours DMEM was removed, the plates were washed with PBS and 1 ml of fresh DMEM without FBS (100 U/ml penicillin, and 0.1 mg/ml streptomycin) was added. Cells were starved for 10-12 hours and then incubated in the presence or absence (control samples) of 1µg/ml of LPS for the indicated time periods. Upon endpoints wells were washed with ice cold PBS and lysed via the addition of 0,5 ml Trizol and RNA was isolated according to manufacturer's instructions. The reverse transcription (using 1 µg isolated RNA as template) and real time PCR reaction was performed with the Invitrogen SuperScript[™] III Platinum[®] Two-Step qRT-PCR Kit with SYBR[®] Green kit according to manufacturer's instructions. Primer pairs used for amplification are listed as follows: IRAK-M, sense: 5' CTT CCC ACT TGA GGT GAA GC 3' and antisense, 5' ATG CTT GGT TTC GAA TGT CC 3', resulting in a 236bp product; for β-actin, sense, 5' TCA GAA GGA CTC CTA TGT GG 3' and antisense, 5' TCT CTT TGA TGT CAC GCA CG 3', resulting in a 499bp product. Amplification was performed in an ABI PRISM 7000 Real- Time PCR apparatus for a maximum of 45 cycles, as follows: 45 s at 95°C, 45 s at 59°C, and 45 s at 72°C. No by-products were present in the reaction, as indicated by the dissociation pattern provided at the end of the reaction. The amplification efficiency of the mouse IRAK-M product was the same as the one of actin, as indicated by the standard curves of amplification, allowing us to use the formula: fold difference = $2^{-(CtA - CtB)}$, where Ct is the cycle threshold. Reactions were performed in duplicates, to allow for statistical evaluation.

4. Chromatin immunoprecipitation.

5 million RAW 264.7 macrophages were plated in 100mm dishes containing 10ml DMEM (10% FBS, 100 U/ml penicillin, and 0.1 mg/ml streptomycin). After 48 hours, DMEM was removed, the plates were washed with PBS and 10 ml of fresh DMEM without FBS (100 U/ml penicillin, and 0.1 mg/ml streptomycin) was added. Cells were starved for 10-12 hours.

For the LPS stimulation assay, the starved RAW 264.7 mouse macrophages were incubated either in the presence or absence (control sample) of 1 μ g/ml of LPS (directly added to the starvation culture medium) for an additional 3h hours. In assays where wortmannin was used, cells were incubated in the presence of both 1 μ g/ml LPS and 100nM/ml wortmannin for the same 3h long period. For the induction of tolerance assay, cells were treated as previously described. In brief, upon the 12 hour starvation, cells were incubated in DMEM+10%FBS +1%Penstrep+ 1 μ g/ml LPS for 12 hours. Plates were then emptied of culture medium, washed with PBS and new DMEM+10%FBS+100 U/ml penicillin, 0.1 mg/ml streptomycin was added. Cells rested in these conditions for 3 hours and then incubated in the presence or absence of 1 μ g/ml LPS for an additional 3 hours.

Upon endpoints, crosslinking of nucleoprotein complexes was achieved with the addition of formaldehyde (1.1 ml from a 10% stock - final concentration 1%) directly into the medium. Samples were then incubated for 20 minutes at 37°C, before quenching the crosslinking reaction via the addition of glycine (0.58ml from a 2.5M stock - final concentration 0.125M) again directly into the medium. After 5 min of incubation in room temperature, the medium was removed and cells were scraped and collected in 7 ml of ice cold PBS supplemented with 1mM PMSF. Cells were washed twice in ice cold PBS/1mM PMSF, resuspended in 1,2 ml of Lysis Buffer and kept on ice for 10 minutes. Samples were either frozen at -80°C at this point or sonicated as follows.

Lysis Buffer : 1% SDS, 10mM EDTA, 50mM Tris Base ph 8

Sonication was performed directly in the lysis buffer suspension. In total 10-15 repeats of 30 second duration were performed on ice, with 5 minute long cool-off intervals. Sonicator intensity was set at 50%. After Sonication, samples were centrifuged twice at 12.000 rpm, 4oC for 15 minutes. Cellular debris was discarded and supernatant, containing the crude soluble chromatin (CSC) was stored at -80°C. On the same day, beads for CSC preclearing were prepared. In brief, 2 eppendorf tubes containing 20 μ l of protein G sepharose beads, were prepared for each CSC sample. The beads were washed 3 times in 0,5ml 1XRIPA buffer/1mM PMSF (Centrifuge at 3500 rpm,4oC for 2 minutes) and blocked overnight in 0,48 ml of fresh blocking buffer, on a rotator at 4oC.

2X RIPA buffer: 2% Triton X-100, 0,2% DOC, 280mM NaCl

Blocking Buffer: 50% 2X RIPA buffer, 1mg/ml BSA, 0,1mg/ml salmon sperm

Verification of successful sonication was performed as follows: 50 μ l of CSC was supplemented with 150 μ l dH₂O and 10.5 μ l of 4M NaCl and the mixture was heated overnight at 65oC in order to reverse crosslinking of nucleoprotein complexes. On the following day the mixture was subjected into RNaseA treatment, phenol/chloroform/isoamylalcohol (PCI) nucleic acid extraction and ethanol mediated,

carrier-assisted (glucogen) nucleic acid precipitation as commonly performed. Precipitated chromatin was diluted in 20µl TE, quantified via Nanodrop measurement, whereas 1-2 µl were subjected to 1.5% gel electrophoresis. Successful sonication was verified when CSC smear exhibited sizes between 500 to 1000bp.

Upon verification of successful sonication, blocked beads for preclearing were spun down (centrifuged at 3500 rpm, 4°C for 2 minutes), and the supernatant was discarded. 5µg of each CSC sample were separately kept at -80°C as input samples, whereas 25µg of CSC from each sample was loaded into either eppendorf tube containing the blocked beads and was supplemented with 250µl 2X RIPA/2mM PMSF/complete protease inhibitors and dH2O up to a total volume of 500µl. In this way two identical mixtures per CSC sample were created. Eppendorfs containing these mixtures were rotated at 4°C for 2 hours, then centrifuged at 3500 rpm, 4°C for 2 minutes and supernatants, containing the precleared CSC were transferred to new tubes. Again in this way, two identical precleared fractions of each CSC sample are created. 5 µg of antibody against the investigated transcription factor (either NF-κB-p65 or C/EBPβ, both purchased from Santa Cruz Biotechnology) were added to one of these fractions, whereas 5 µg against anti Chromomin (not a transcription factor) were added to the other, in order to estimate non specific binding by the beads (internal negative control). Binding of the antibody was facilitated via overnight rotation at 4°C.

On the same day, beads for precipitation were prepared in exactly the same fashion as the beads for the preclearing.

On the next day, the blocked beads (complete mixture) and the CSC-Ab samples were combined. The combined solution was rotated for 2 hours at 4°C. At endpoint, beads were spun down and washed 7 times with 1ml 1X RIPA wash buffer/ 1mM PMSF. The beads pellet was then dissolved into 100µl TE/0,5% SDS and 2 µl of Proteinase K from a 10mg/ml stock was added into each sample. Mixtures were then incubated for 3 hours at 55°C and then overnight at 65°C. The same process was followed for input samples too: upon thawing, they were diluted up to 120 µl with TE /0,5% SDS and 2 µl of Proteinase K (10mg/ml stock) and incubated with the rest of the samples overnight.

2X RIPA wash buffer: 2% Triton X-100, 0,2% DOC, 0,2% SDS, 1M NaCl

The following morning RNase A treatment (0,5µl RNase A from a 20mg/ml stock per sample, 30 min incubation at 37°C), PCI nucleic acid extraction and ethanol precipitation with 20µg glucogen per sample were performed. DNA pellets were resuspended in 50µl TE buffer.

Data analysis was performed via either via low cycle (30) cycle PCR amplification or real time PCR (or both), using 5µl of the precipitated chromatin for each reaction. Primers used for these assays are noted in **Box 3**.

Site	Sense	Antisense	Length (bp)
Distal κB (-1099 bp)	F2 : 5' AGC CGA GCT GAG ACA TTG GGG TCA AGC AAC 3'	Rev4: 5' ACA CCCC AAA AAG GGT CTC T 3'	245
Proximal κB (-339bp)	F4n: 5' CCT GAC GGG ACA AAG AGA AA 3'	Rev7: 5' CAC CCC AGG TCA TCT TTG TTA 3'	217
Distal C/EBP (-480bp)	F3 : see Box1 used for cloning	Rev6: 5' TTT AAA CGG AAG GAA ACG TG 3'	293
Proximal C/EBP (-79 and -110 bp)	F4n: 5' CCT GAC GGG ACA AAG AGA AA 3'	R2: see Box1 used for cloning	409

Box 3

For quantitative analysis via real time PCR, the Ct of each positive sample (precipitated chromatin with specific antibody - Ct+) was compared to the Ct of the background sample (non specific antibody - Ct-) as fold difference = $2^{-(Ct+ - Ct-)}$, in the context of similar Cts for input samples (total sonicated chromatin).

C. Results

A. Online data mining and in silico analysis of upstream irak3 sequences

A1. Data available in public online databases

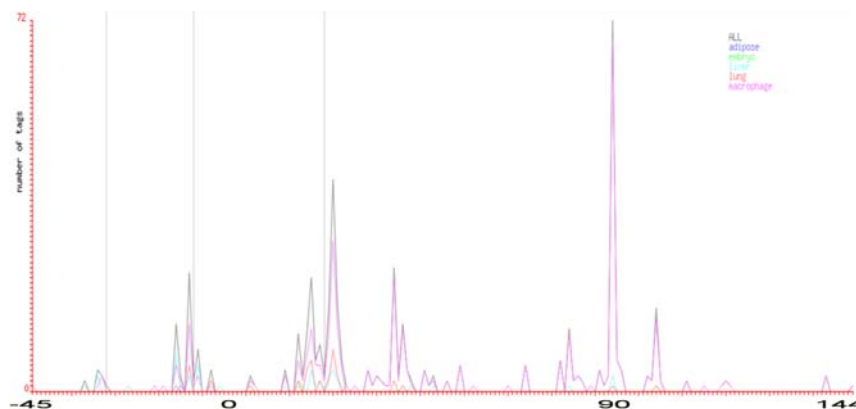
In our efforts to characterize irak3's (geneID 73914) core promoter and regulatory elements, focus was placed on sequences directly upstream of irak3's first mapped exon.

To gain understanding on irak3 transcription, the Gene and Genomatix public online databases were investigated for the existence of different irak3 mRNAs. Data mining revealed the existence of 5 different transcripts containing the first exon along with upstream non coding sequences. Transcripts exhibiting gaps in the 1st exon and upstream sequences (AK028436, AJ440757.2) were excluded from the search. Findings are summarized in box1.

cDNA Accession	Mouse strain	Transcript length in bp	5' UTR length in bp	Tissue
AK014783	C57BL/6J	1171	128	0 day neonate head
AK029057	C57BL/6J	2969	78	10 day neonate skin
AK049210	C57BL/6J	1957	109	ES cells
AF461763.1	C57BL/6J	1888	58	BMDM
BC120829.1 BC120831.1 BC144835.1	unknown	2421	39	testicles
NCBI reference: NM_028679				
Box4: a list of all known transcripts that retain the 1 st exon without sequence gapping				

As shown in **Box 4**, the 5' UTR exhibited significant variability among transcripts. Since a careful definition of the transcription start site (TSS) could illuminate transcription factor coupled irak3 transcription (and probably exclude putative binding sites), the Genomatix and DBTSS public databases were investigated for putative known TSSs.

As shown in **Picture 2**, experimental data from Cap-analysis gene expression (CAGE), acquired from the Genomatix database, attribute the highest number of tags in murine macrophages at a site located approximately 90 bp upstream of the translation start site. It is also noteworthy that a smaller peak of tags can be found in a region just 30



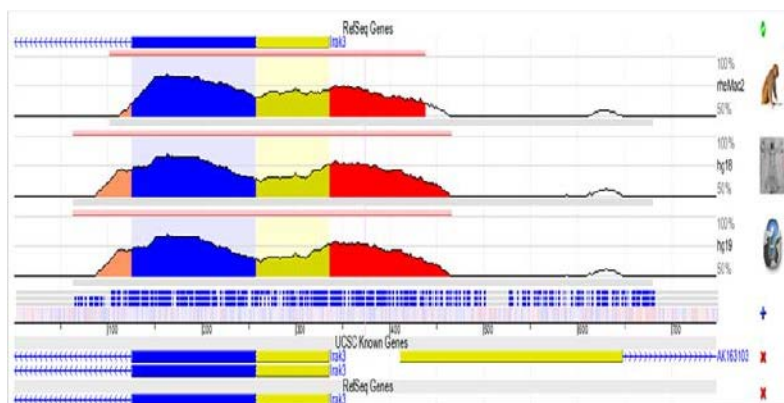
Picture 2. Experimental data from Genomatix database reveal the existence of at least 2 putative transcriptional start regions located approximately 30 and 90 bp upstream of the translation start site .

bp approximately upstream of the known translation start site. Moreover, data retrieved from the DBTSS online database, derived by similar methods to CAGE (oligo-capping), show a total of 11 putative TSSs, out of which 4 are located in close proximity in a region approximately 110 bp upstream from the known translation start site (**Picture 3**).



Picture 3: as retrieved from the online DBTSS. 11 TSS are recognized via the oligo capping method.

Whereas, 5' RACE-PCR was not performed for TSS characterization in our background, these data available online hint towards the initiation of irak3 transcription at a site located approximately 90-100 base pairs upstream of ATG. This notion is also supported by cross



Picture 4: As retrieved from the ECR Browser website. Cross species homology study identifies a well conserved 150 bp long region just 80 bp upstream of the translation start site

species homology observations. As shown in **picture 4** (acquired from ECR browser), the highest level of non coding sequence conservation between humans, mouse and Rhesus Macaque must be attributed to a 150 bp region just upstream of the NM_028679's (transcript of NCBI reference) 5' UTR and approximately 80 bp upstream of the known ATG. This 150 bp region should serve as a prime candidate for irak3 core promoter characterization.

A2. In silico analysis of the sequence upstream of irak3

Two search engines, Genomatix and TFsearch, both available online, were used for in silico analysis of upstream sequences. Special focus was attributed to the transcription factors that are presented below, along with bibliographical evidence putatively linking them to IRAK-M transcription:

NF- κ B: the classical pathway for NF- κ B activation is induced by TLR signaling. Moreover tpl2 has been shown to activate this transcription factor via NIK/IKKa/IKb[51] and MSK1[52] dependent mechanisms. Likewise, Akt1 is able to activate IKKa and p65 via NIK[53].

AP-1: is known to be induced by various MAPKs among which ERK and JNK, downstream effectors of TLR signaling.

PU.1: stably expressed in cells of monocytic origin. Phosphorylated by Akt[54]. Imperative for IRAK-M transcription.

C/EBP β : Akt dependent dephosphorylation of C/EBP β promotes its transcriptional efficacy[55].

SMADs: downstream effectors of TGF β signaling.

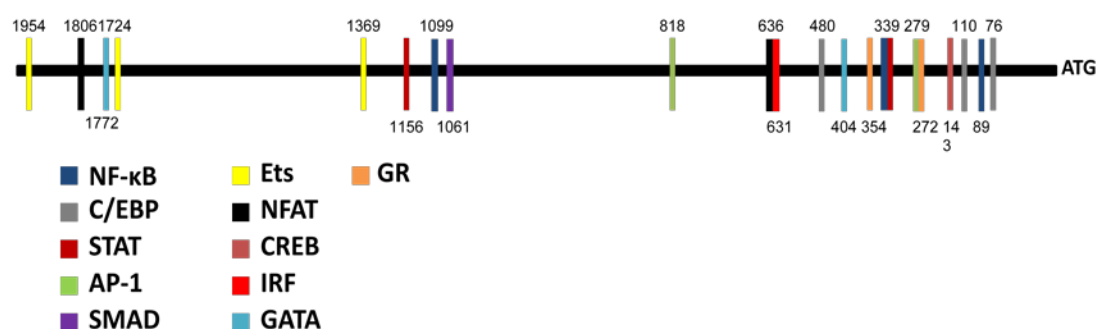
GR: glucocorticoids have been shown to regulate IRAK-M expression [45].

The results of the combined search by these two databases are briefly portrayed in **picture 5**. Numbering is relative to the translation start site.

Analysis showed that irak3 is a TATA-less gene. Moreover no consensus Inr and DPE sites could be identified. However, a number of putative transcription factor binding sites were revealed and served as the basis for further programming.

Remarks

- Significant clustering of putative binding sites is exhibited proximally to the 1st exon.
- A very attractive transcription factor module comprised of a κ B motif and a C/EBP site (at 89bp and 76bp respectively) might not be considered as functional, since their sequences are commonly found to be part of the 5' UTR in IRAK-M transcripts.
- A non-consensus κ B motif is overlapping with a GAS motif for STAT transcription factors approximately 339 bp upstream of the translation start site.
- 3 κ B and 3 C/EBP sites were identified in total.

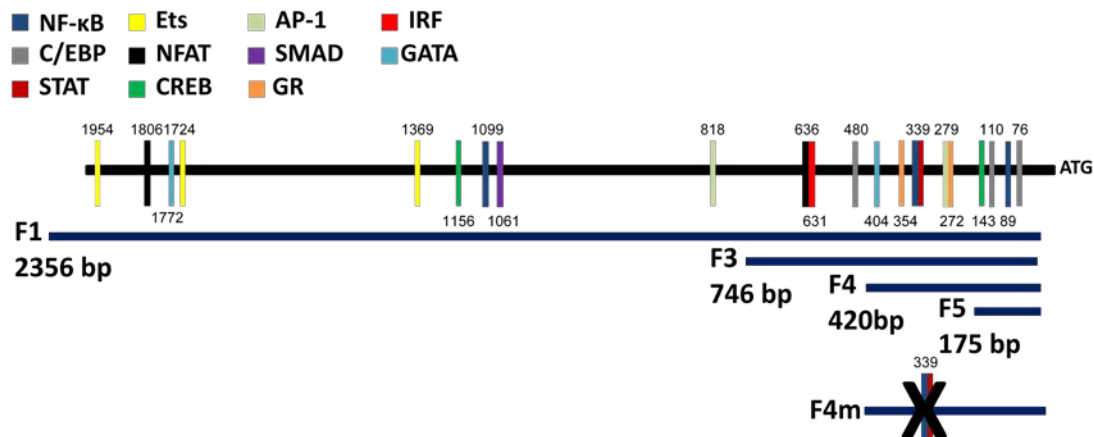


Picture 5: in silico analysis of irak3 upstream sequence as performed by the Genomatix and TFsearch online engines

B. Experimental assays

Upstream sequences of irak3 respond to LPS stimulation

In order to assess the ability of upstream sequences to drive irak3 expression, we cloned 4 5' sequences of different length into the pgl3basic vector, bearing the firefly luciferase reporter gene. Thus, 4 reporter plasmid constructs were created and named F1, F3, F4 and F5. Insert lengths corresponding to each reporter plasmid are visualized in **picture 6**. Another construct, bearing the F4 insert mutated for the overlapping NF-κB and Stat binding sites, (located approximately 339 bp upstream of the translation start site) was provided by Zacharioudaki V. Point mutations in this construct, termed F4m, disrupted both binding sites.



Picture 6 : relative sizes of each insert are shown. F4m contains a mutated F4 insert sequence, in which two overlapping binding sites (one for NF-κB and one for STAT factors) are disrupted.

These constructs were transiently transfected into RAW 264.7 mouse macrophages, as described in materials and methods. Mock and empty vector samples were also included.

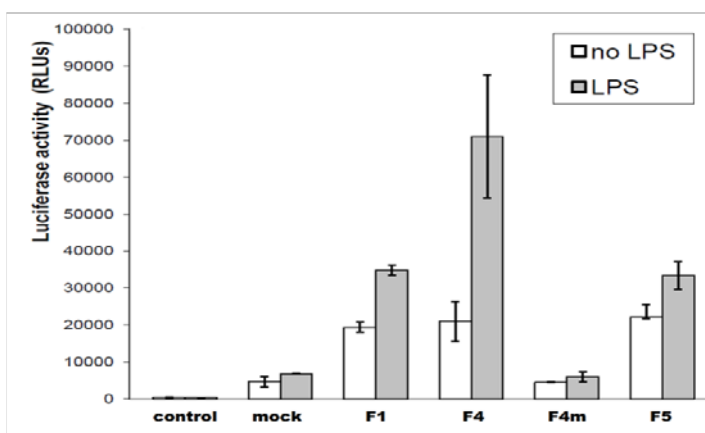


Figure 1: Mutations in overlapping STAT and NFκB binding sites, halts LPS mediated IRAK-M transcription

RAW 264.7 mouse macrophages were transiently transfected (via electroporation) with 6μg of F1, F4, F5 or Fm constructs and stimulated in starvation medium with or without 1μg/ml of LPS for 24 hours. Luciferase activity is measured in Relative Luciferase Units. Standard error bars account for three different transfection samples.

The transfected cells were incubated in the presence or absence of 1μg/ml LPS. Upon 24 hours they were lysed and luciferase activity was measured in each sample. A 24 hour incubation period was selected for adequate luciferase protein accumulation. Stimulation was

performed in culture medium without FBS.

As shown in figure 1, LPS is able to induce luciferase transcription in RAW 264.7

mouse macrophages, transfected for each of the F1, F4 and F5 constructs. Thus, transcription factors downstream of TLR4 signaling could possibly drive IRAK-M expression, by functioning unto sequences directly upstream of the *irak3* gene. Moreover, the highest luciferase activity was elicited when cells were transfected for the F4 construct. This effect was lost and transcription was halted when two overlapping binding sites, one for NF- κ B and

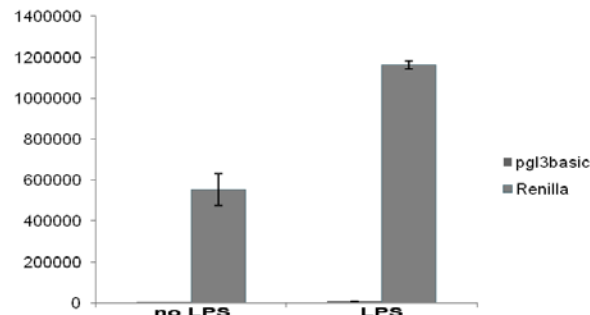


Figure 2: LPS induces Renilla luciferase transcription.

Upon co-transfection in RAW 264.7 mouse macrophages of 6 μ g of an empty pgl3basic vector and 3 μ g of Renilla luciferase reporter, a 24-hour stimulation with 1 μ g/ml LPS is able to induce Renilla luciferase transcription. Reporter activity is stated in Relative luciferase units (RLUs).

activities when empty pgl3basic vector and the Renilla construct are co-transfected into RAW 264.7 mouse macrophages. As shown, LPS is able to promote Renilla luciferase transcription and thus Renilla activity cannot produce a reliable measure of transfectability

under these conditions. Normalization in subsequent experiments is performed according to total protein concentration as measured via Braddford.

It has to be noted however that normalization for these samples was not possible via renilla luciferase co-transfection: Figure 2 shows the relative firefly and Renilla luciferase

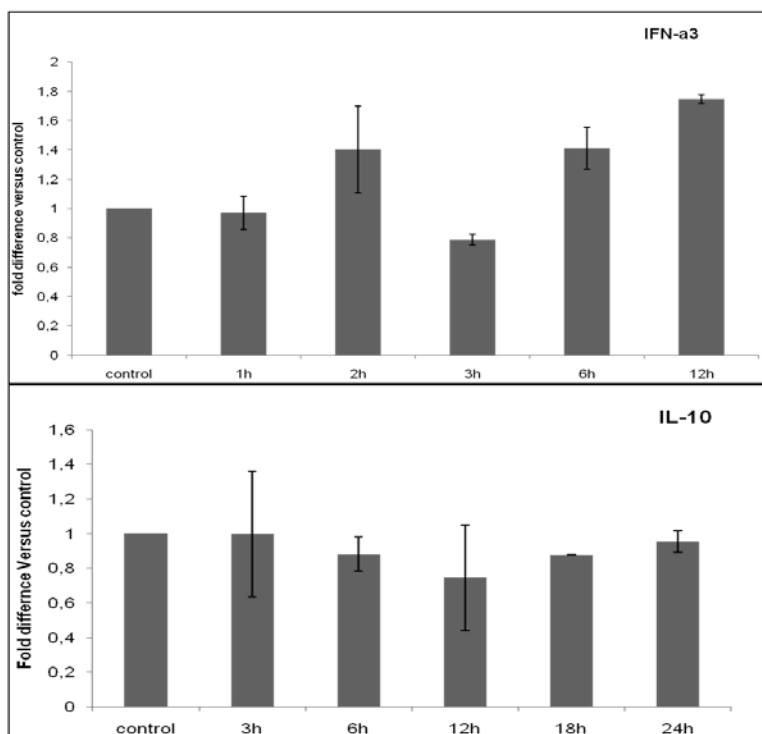


Figure 3: IFN-a3 and IL-10 do not regulate IRAK-M expression

Starved RAW 264.7 mouse macrophages were incubated in the presence or absence (control sample) of 100 IU/ml of IFNA-a3 (figure 3a) or 10ng/ml of IL-10 (figure 3b) for high time points. IRAK-M expression is measured via real time RT-PCR. Relative expression is shown as compared to the control sample. Data are representative of 2 experiments.

under these conditions. Normalization in subsequent experiments is performed according to total protein concentration as measured via Braddford.

IFN-a3 and IL-10 do not upregulate IRAK-M

Since, *irak3* transcription was shown to be dependent on either the κ B or the GAS motif found approximately 339 bp upstream of the translation start site, we hypothesized that either fast acting, NF- κ B dependent or slow progressing, STAT dependent transduction was taking place during this gene's expression (or

putatively both). Elaborating in STAT dependent mechanisms, we theorized that IRAK-M transcription could progress in an autocrine/paracrine dependent fashion during the 24 hours of LPS stimulation.

Both IFN- α [61] and IL-10[60] have been shown to be produced and secreted by macrophages during LPS stimulation. The former, upon receptor binding, confers mainly STAT1 activation whereas the latter STAT3 activation. Thus, RAW 264.7 mouse macrophages were (or weren't) stimulated in vitro with either recombinant IFN- α 3 or recombinant IL-10 for high timepoints. On endpoints cells were lysed, RNA isolated and IRAK-M transcription evaluated via qRT-PCR. As shown in **figure 3 (a and b)**, neither 10ng/ml of IL-10 (in a time course of 24 hours) or 100 IU/ml of IFN- α 3 (in a timecourse of 12 hours) are able to induce IRAK-M transcription.

IFN- α 3 and IL-10 are also unable to confer irak3 promoter activation: In 5 separate experiments (**figure 4**), RAW 264.7 mouse macrophages were transiently transfected with each of the F1,F3,F4,F5 and F4m reporter plasmids (one plasmid per experiment) and were

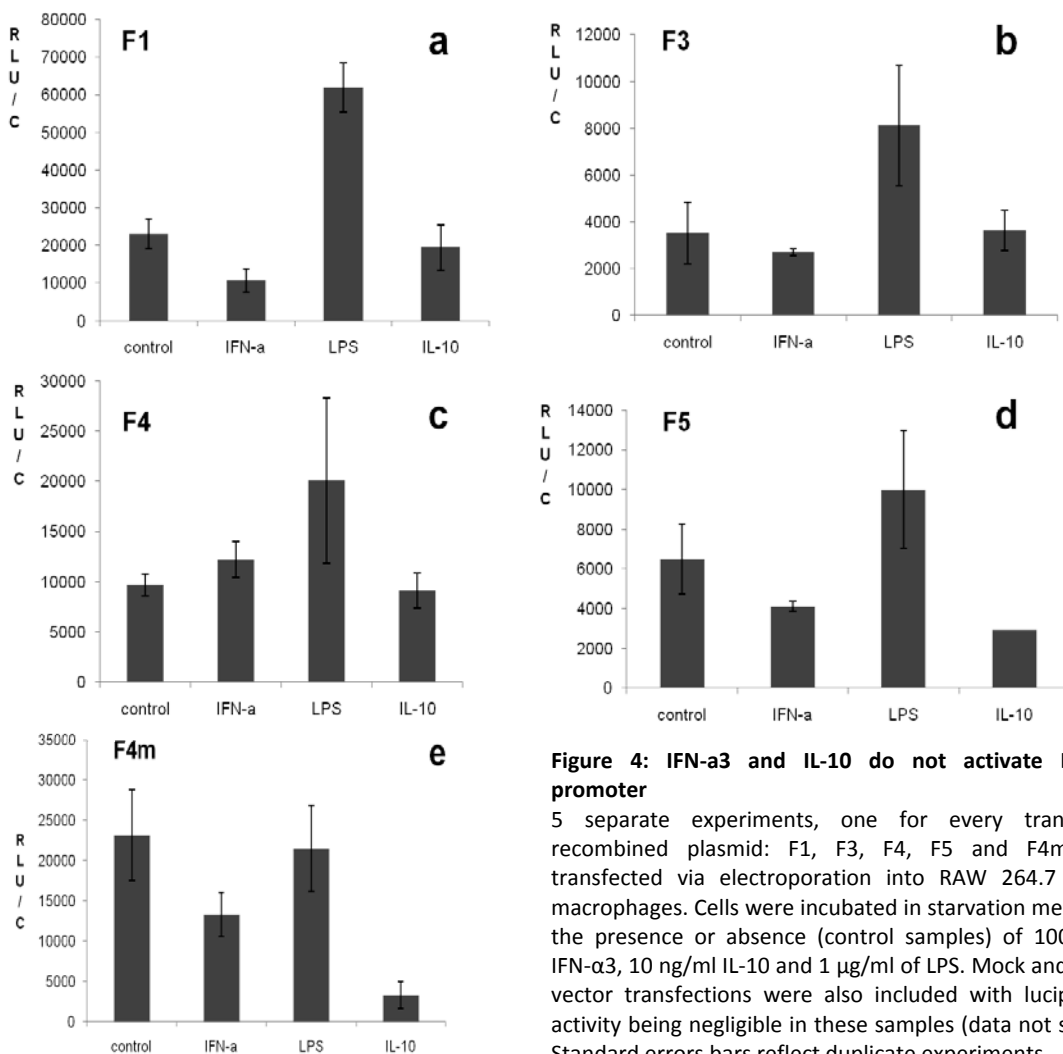


Figure 4: IFN- α 3 and IL-10 do not activate IRAK-M promoter

5 separate experiments, one for every transfected recombinant plasmid: F1, F3, F4, F5 and F4m were transfected via electroporation into RAW 264.7 mouse macrophages. Cells were incubated in starvation medium in the presence or absence (control samples) of 100 IU/ml IFN- α 3, 10 ng/ml IL-10 and 1 μ g/ml of LPS. Mock and empty vector transfections were also included with luciferase activity being negligible in these samples (data not shown). Standard errors bars reflect duplicate experiments.

incubated in the presence or absence of either 10ng/ml IL-10, 100IU/ml IFN- α 3 or 1 μ g/ml LPS for 24 hours. Mock and empty vector transfections also took place. As exhibited in **figure 4a-d**, both IL-10 and IFN- α 3 were unable to increase luciferase transcription in macrophages transfected with any of the recombined plasmids. On the other hand, the ability of LPS to upregulate IRAK-M is evident across all experiments utilizing non mutant constructs. However, LPS induction is again abrogated and comparable to the control samples when cells are transiently transfected for the mutant construct F4m.

It has to be noted that RAW 264.7 cells are particularly resistant to electroporation mediated delivery of foreign DNA. In the absence of a proper method to evaluate transfectability (the Renilla promoter was previously shown to respond to LPS stimulation), variability in each sample is to be expected. However, whereas separate experiments might not be used for direct comparison, the net effect of LPS in upregulating IRAK-M in each of the transfected constructs, should not be underestimated.

Binding of NF- κ B in predicted sites of IRAK-M promoter

As previously shown, LPS is able to promote IRAK-M expression in vitro reporter assays. This is also consistent with reports showing LPS conferred IRAK-M upregulation in ex vivo[8,36] backgrounds. Thus, in our efforts to characterize transcription factors regulating this process, we focused on transcription factors directly downstream of LPS-TLR4 signaling.

NF κ B is probably the most critical mediator of LPS-TLR4 signalling. Upon activation it is released from the cytoplasm, enters the nucleus and drives the expression of several genes that govern an inflammatory response.

In total, 3 κ B motifs can be found in upstream sequences of irak3: One located at -89 bp, one at -339bp overlapping a GAS motif and one at -1099bp. As previously shown in the reporter assays, point mutation disrupting the second κ B motif located at -339bp were able to

abrogate LPS induced IRAK-M upregulation. Thus, we went on to exhibit physical binding of NF- κ B on this site.

Starved RAW 264.7 mouse macrophages were stimulated for 3hours with LPS and chromatin immunoprecipitation assay

was carried out utilizing a mouse Ab for the p65 (RelA) subunit of active NF- κ B. Binding on the κ B motif located 339 bp upstream of the translation start site is shown by the quantitative amplification of a 220 bp sequence that contains it.

As shown in figure 1(a,b), 3

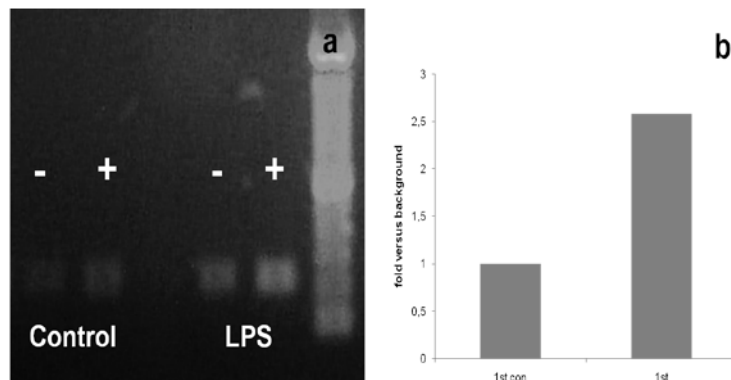
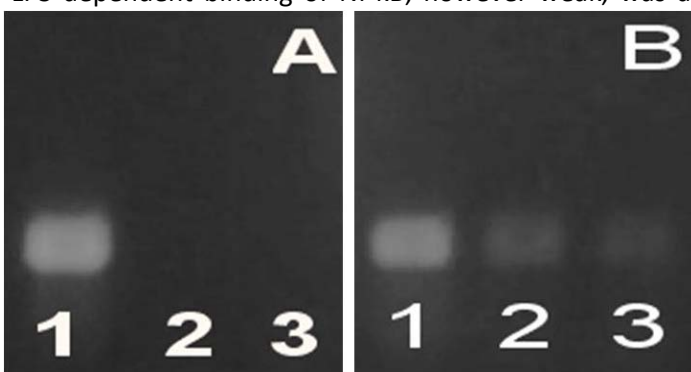


Figure 5. LPS promotes binding of NF κ B at the κ B site located 339 bp upstream of the translation start site.

An antibody with specificity against p65 was used (or not – internal control sample) to precipitate the NF- κ B responsive chromatin from starved RAW 264.7 mouse macrophages incubated in the presence or absence (control sample) of LPS for 3 hours. 25 μ g of sonicated chromatin was used for each precipitation. **Figure 5a**. Binding is exhibited via a 30 cycle PCR amplification of a 220 bp long sequence containing the putative binding site. - : no Ab used - assay background; + : Ab used– specific chromatin. **Figure 5b**. Binding is exhibited by real time PCR amplification. Results for each sample are versus the internal control samples (no Ab used). Data are representative of at least 3 experiments.

hours of LPS stimulation induces approximately 2,6 times more binding as compared to the control sample (no LPS stimulation). Data are representative of at least 3 experiments.

LPS dependent binding of NF- κ B, however weak, was also exhibited for the distal κ B site,



located 1099bp upstream of the translation start site (**Figure 6**). Concerning the proximal predicted binding site, located at -89bp, the probability of it being functional was ruled out since sequences that comprise it are shown to be part of the 5' UTR in several IRAK-M transcript

(**Box2**).

Figure 6. LPS induced weak binding of NF- κ B on the distal predicted NF- κ B site.

Chromatin immunoprecipitation using an anti p65 antibody, was performed to precipitate NF- κ B responsive chromatin from LPS treated and untreated RAW 264.7 mouse macrophages. Binding is exhibited via a 30 cycle PCR amplification of a 245 bp long sequence containing the putative binding site, located 1099 bp upstream of the translation start site. 12 hours of LPS induction is able to promote NF- κ B binding (**Figure 1B**) as opposed to untreated cells (**Figure 1A**): **1**: total sonicated chromatin; **2**: no Ab used - assay background; **3**: Ab used - specific chromatin. Data are representative of two separate experiments.

LPS induced binding of C/EBP β

It is well established that LPS is able to promote the activation of the PI3K-akt signaling cascade in mouse macrophages. Moreover, this phenomenon is thought to function as a limiting mechanism towards LPS signaling, creating an internal inhibitory loop that limits excess activation. Thus, in recent publications the PI3K-akt1 axis has been shown to be a key effector of endotoxin tolerance, functioning through diverse mechanisms [9,67], among which the upregulation of IRAK-M[36].

In our efforts to explain this effect of PI3K-akt1 axis onto IRAK-M expression we investigated whether CCAAT enhancer binding protein β (C/EBP β), a transcription factor regulated by akt responses is able to affect this gene's transcription. Moreover, according to the in silico analysis, predicted C/EBP sites were found proximally to *irak3*'s transcription start sites, making this transcription factor a significant candidate of IRAK-M's regulation. In total 3 predicted C/EBP binding sites were predicted: two proximal located at 76bp and 110 bp upstream of the translation start site and one distal at -480bp.

Starved RAW 264.7 mouse macrophages were either stimulated for 3 hours with 1 μ g/ml LPS or rendered tolerant (-via a 12 hour long stimulation with 1 μ g/ml LPS) and then restimulated for another 3 hours with 1 μ g/ml LPS. Chromatin immunoprecipitation assay was carried out in these samples, utilizing a mouse Ab for C/EBP β .

Whereas no significant binding was exhibited for the distal binding site (data not shown), the proximal ones produced significant binding, both in the first LPS stimulation and under conditions of tolerance, as shown in **figure 7a** and **7b**. Moreover when starved RAW 264.7 mouse macrophages were incubated for 3 hours in the presence of both LPS and wortmannin (an inhibitor of PI3K signaling), C/EBP β binding was severely reduced (**Figure 7b**). Thus it,

should be concluded that IRAK-M transcription is C/EBP β dependent, whereas PI3K regulates this process functioning in favor of a tolerogenic phenotype.

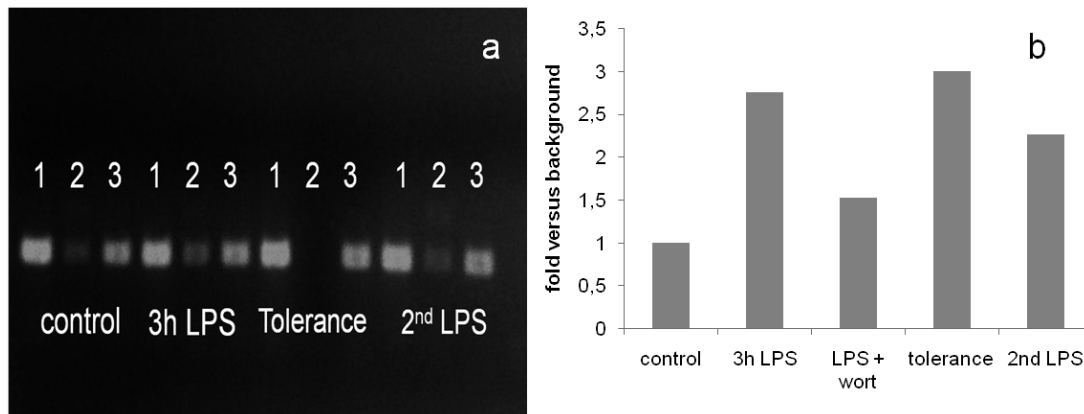


Figure 7: LPS promotes PI3K/akt dependent binding of C/EBP β in sites proximal to the translation start sites
 Starved RAW 264.7 mouse macrophages were either stimulated for 3hours with 1 $\mu\text{g}/\text{ml}$ LPS (**3h LPS**) or rendered tolerant –via a 12 hour long stimulation with 1 $\mu\text{g}/\text{ml}$ LPS and then restimulated for another 3 hours with 1 $\mu\text{g}/\text{ml}$ LPS (**2nd LPS**) or not (**Tolerance**). In these samples chromatin immunoprecipitation assay utilizing a specific antibody against C/EBP β was performed and 25 μg of sonicated chromatin from each sample. **Figure 7a:** binding is exhibited via a 30 cycle PCR amplification of a 409 bp long sequence containing the putative binding site. **1:** total sonicated chromatin; **2:** no specific Ab used - assay background; **3:** specific Ab used – specific chromatin. **Figure 7b:** An additional sample in which starved RAW 264.7 mouse macrophages are incubated in the presence of both 1 $\mu\text{g}/\text{ml}$ LPS and 100nM/ml wortmannin (**LPS + wort**). Binding is exhibited by real time PCR amplification. Results for each sample are versus the internal control samples (no Ab used). Data are representative of 2 experiments, except the **LPS + wort** sample, which is a single experiment.

Lastly, it should be noted that a distinction between the two proximal C/EBP binding sites, at the level of chromatin immunoprecipitation cannot be made, since both sites are located in close proximity. We are currently in the process of verifying binding both for the NF- κB and the C/EBP sites mentioned, via EMSA in vitro. In vitro binding assays should be able to show which of the two sites is responsible for C/EBP β binding. However, it should be noted that the C/EBP site located at -76 is an unlikely candidate, because sequences that comprise it have been found to belong to IRAK-M's 5' UTR.

D. Discussion

Ever since 2002, IRAK-M is considered to be closely linked with the adaptation of endotoxin tolerance in cells of the innate immunity. Functioning as a physiological dominant negative isoform in the IRAK family of kinases, it abrogates signal transduction downstream of TLR4 receptor and limits excess inflammatory responses. However, whereas there is a relatively good understanding of its function, its regulation still remains a mystery.

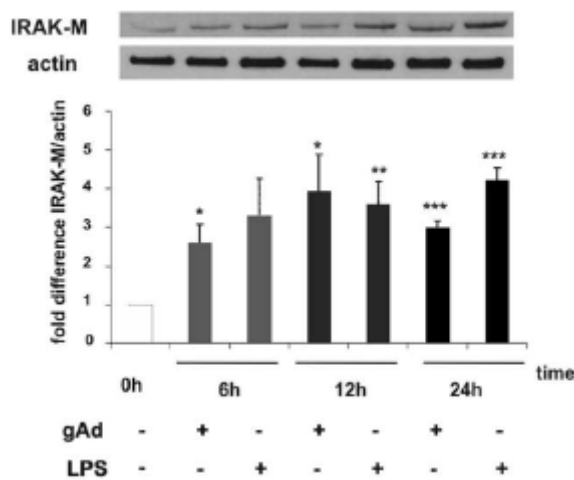


Figure 8: both adiponectin and LPS induce IRAK-M expression in primary mouse macrophages.

As adapted by Zacharioudaki V et al 2009[36]

Over the years it has become well understood that LPS (among other TLR ligands), is a strong inducer of IRAK-M expression. The kinetics of this phenomenon are complex: As shown in Figure 8, adapted from Zacharioudaki et al 2009 [36], IRAK-M protein levels increase sharply upon LPS induction, peak at 12 hours and remains high even after 24 hours of continued LPS stimulation. Such a phenomenon can only partly be attributed to fact acting transcriptional

mediators, such as NF- κ B.

In this study, we have summarize available online data concerning irak3

transcription and perform an in silico analysis of the upstream sequence, in order to identify putative transcription factor binding sites. We dissect the upstream sequences of the irak3 gene to functionally test their relevance in IRAK-M expression and provide for the first time evidence of physical transcription factor binding on irak3 promoter.

As evidenced by the in silico analysis irak3 is a TATA-less gene. Typical Inr and DPE sites are also not identified. However a significant clustering of relevant transcription factors can be found starting approximately 80-100 bp upstream of the translation start site. This correlates well with an abundance of online data attributing the TSS in a region 90-100 bp upstream of the first exon.

Of particular interest was a non consensus NF- κ B site (-consensus sequence is disrupted in just the second 5' nucleotide) overlapping with a GAS motif for STAT factor binding. Mutation of both binding sites led to a significant decrease in luciferase expression upon LPS stimulation, providing evidence that this region is critical for irak3 transcription.

Both IL-10[60] and type I interferons[61] are secreted by macrophages upon LPS treatment. Cellular signaling by IFN- α follows mainly a STAT1 dependent pathway, whereas IL-10 opts for STAT3 activation [62]. However, neither IFN- α 3 nor IL-10 are able to upregulate IRAK-M. This suggested that this region is mainly NF- κ B responsive. As shown via chromatin immunoprecipitation assay, NF κ B is able to bind in this particular region upon LPS stimulation.

However, a functional role for STAT mediated signaling should not be excluded. Whereas IFN- α 3 and IL-10 do not upregulate IRAK-M, either of them could possibly downregulate it, but only in the context of LPS stimulation: Transcription factor competition for promoter

binding is a well established mechanism for gene regulation [59]. Thus, an autocrine/paracrine function for IFN- α , IL-10 in repressing NF- κ B mediated transcription and limiting irak3 expression, should not be excluded yet. Regrettably, co-stimulation assays with IFN- α 3/IL-10 and LPS that could illuminate this possibility are still pending.

NF- κ B on the other hand is shown to be able to promote IRAK-M expression. Such fast NF- κ B mediated responses should be critical in the rapid upregulation of irak3. However upon tolerogenic conditions, where NF- κ B activation should be minimal, other transcription factors could confer IRAK-M expression and keep it at high levels.

C/EBP β is a member of the CCAAT-enhancer binding proteins, containing a leukine zipper motif. It is inducible by various inflammatory stimuli among which LPS [63] and is known to collaborate with NF- κ B in the regulation of many genes [64,65,66]. Moreover, C/EBP β function has been repeatedly shown to be PI3K/akt regulated [55].

Again with chromatin immunoprecipitation assay we show that C/EBP β can bind at sites directly upstream of irak3. This is an effect that upon tolerogenic conditions is still strong and putatively drives IRAK-M expression. Finally, this effect is shown to be PI3K regulated, in accordance to publications derived from our laboratory, according to which globular adiponectin is able to induce IRAK-M transcription via PI3K/akt regulated mechanisms[36]. It should be noted however, that currently this prime effect of PI3K/akt signaling in C/EBP β transactivation is unknown. It could account to either C/EBP β phosphorylation status, or the predominance of either LAP or LIP C/EBP β isoform[68]. Both mechanisms are known to be affected by PI3K/akt signaling.[55,68]

In conclusion, data accumulated so far point towards a basic concept in gene regulation: signaling pathways lead their own inactivation. In the case of LPS, signal transduction creates a self afflicting inhibitory loop: TLR4 signaling promotes NF- κ B and C/EBP β activation which in turn leads to the intracellular accumulation of a potent negative regulator, IRAK-M.

F. Future prospects

Here we show that IRAK-M transcription is NF- κ B and C/EBP β regulated. However, the story of IRAK-M expression is far from over. As noted in the introduction, molecules other than the classic effectors of inflammation have been shown to regulate its expression. Such molecules include hormones –glucocorticoids, or even cytokines that have an anti-inflammatory effect, such as TGF β . Conversely it would be interesting to investigate the possibility that IRAK-M transcription is not just an after effect of inflammation, but also a closely coordinated procedure regulated by anti-inflammatory stimuli too. Precisely, as exhibited in **picture 5**, during the in silico analysis we identified putative binding sites for both the glucocorticoid receptor and SMAD molecules. Thus the work presented here is just a part of our efforts in identifying IRAK-M core promoter and regulatory elements.

Moreover, IRAK-M immunoregulatory properties should not be restricted only to the context of acute inflammation. Innate immunity is known to have an important part in other processes too such as cancer and tumor progression. Thus, we are currently investigating the effect of IRAK-M expression in myeloid derived suppressor cells, an immature population of myelomonocytic origin that is elicited upon tumor progression and confers a suppressive effect on cells of the adaptive immunity [69]. C/EBP β was recently shown to be invaluable in

the generation of MDSCs[70]. Thus, a putative interplay between IRAK-M, PI3K/akt responses and C/EBP β may exist in MDSC generation and/or function.

Z.References

1. Medzhitov R. Recognition of microorganisms and activation of the immune response. *Nature*. 2007 Oct 18;449(7164):819-26
2. O'Neill, L.A. and Bowie, A.G. (2007) The family of five: TIR-domaincontaining adaptors in Toll-like receptor signalling. *Nat. Rev.Immunol.* 7, 353–364
3. Biswas SK, Lopez-Collazo E. Endotoxin tolerance: new mechanisms, molecules and clinical significance. *Trends Immunol.* 2009 Oct;30(10):475-87
4. del Fresno C, García-Río F, Gómez-Piña V, Soares-Schanoski A, Fernández-Ruiz I, Jurado T, Kajiji T, Shu C, Marín E, Gutierrez del Arroyo A, Prados C, Arnalich F, Fuentes-Prior P, Biswas SK, López-Collazo E. Potent phagocytic activity with impaired antigen presentation identifying lipopolysaccharide-tolerant human monocytes: demonstration in isolated monocytes from cystic fibrosis patients. *J Immunol.* 2009 May 15;182(10):6494-507
5. Medvedev AE, Kopydlowski KM, Vogel SN. Inhibition of lipopolysaccharide-induced signal transduction in endotoxin-tolerized mouse macrophages: dysregulation of cytokine, chemokine, and toll-like receptor 2 and 4 gene expression. *J Immunol.* 2000 Jun 1;164(11):5564-74.
6. Nakagawa R, Naka T, Tsutsui H, Fujimoto M, Kimura A, Abe T, Seki E, Sato S, Takeuchi O, Takeda K, Akira S, Yamanishi K, Kawase I, Nakanishi K, Kishimoto T. SOCS-1 participates in negative regulation of LPS responses. *Immunity.* 2002 Nov;17(5):677-87.
7. Heyninck K, Beyaert R. The cytokine-inducible zinc finger protein A20 inhibits IL-1-induced NF-kappaB activation at the level of TRAF6. *FEBS Lett.* 1999 Jan 15;442(2-3):147-50.
8. Kobayashi K, Hernandez LD, Galán JE, Janeway CA Jr, Medzhitov R, Flavell RA. IRAK-M is a negative regulator of Toll-like receptor signaling. *Cell.* 2002 Jul 26;110(2):191-202
9. Androulidaki A, Iliopoulos D, Arranz A, Doxaki C, Schworer S, Zacharioudaki V, Margioris AN, Tsiglis PN, Tsatsanis C. The kinase Akt1 controls macrophage response to lipopolysaccharide by regulating microRNAs. *Immunity.* 2009 Aug 21;31(2):220-31.
10. Wesche H, Gao X, Li X, Kirschning CJ, Stark GR, Cao Z. IRAK-M is a novel member of the Pelle/interleukin-1 receptor-associated kinase (IRAK) family. *J Biol Chem.* 1999 Jul 2;274(27):19403-10
11. Rosati O, Martin MU. Identification and characterization of murine IRAK-M. *Biochem Biophys Res Commun.* 2002 May 24;293(5):1472-7.
12. Janssens S, Beyaert R. Functional diversity and regulation of different interleukin-1 receptor-associated kinase (IRAK) family members. *Mol Cell.* 2003 Feb;11(2):293-302
13. Ye H, Arron JR, Lamothe B, Cirilli M, Kobayashi T, Shevde NK, Segal D, Dzivenu OK, Vologodskaja M, Yim M, Du K, Singh S, Pike JW, Darnay BG, Choi Y, Wu H. Distinct molecular mechanism for initiating TRAF6 signalling. *Nature.* 2002 Jul 25;418(6896):443-7
14. Wesche H, Henzel WJ, Shillinglaw W, Li S, Cao Z. MyD88: an adapter that recruits IRAK to the IL-1 receptor complex. *Immunity.* 1997 Dec;7(6):837-47.
15. Cao Z, Xiong J, Takeuchi M, Kurama T, Goeddel DV. TRAF6 is a signal transducer for interleukin-1. *Nature.* 1996 Oct 3;383(6599):443-6
16. Jiang Z, Ninomiya-Tsuji J, Qian Y, Matsumoto K, Li X. Interleukin-1 (IL-1) receptor-associated kinase-dependent IL-1-induced signaling complexes phosphorylate TAK1 and TAB2 at the plasma membrane and activate TAK1 in the cytosol. *Mol Cell Biol.* 2002 Oct;22(20):7158-67.
17. Wang C, Deng L, Hong M, Akkaraju GR, Inoue J, Chen ZJ. TAK1 is a ubiquitin-dependent kinase of MKK and IKK. *Nature.* 2001 Jul 19;412(6844):346-51.
18. Suzuki N, Suzuki S, Duncan GS, Millar DG, Wada T, Mirtsos C, et al. Severe impairment of interleukin-1 and Toll-like receptor signalling in mice lacking IRAK-4. *Nature* 2002;416:750–6.
19. Li L, Su J, Xie Q. Differential regulation of key signaling molecules in innate immunity and human diseases. *Adv Exp Med Biol* 2007;598:49–61.
20. Schoenemeyer A, Barnes BJ, Mancl ME, Latz E, Goutagny N, Pitha PM, et al. The interferon

regulatory factor, IRF5, is a central mediator of toll-like receptor 7 signaling. *J Biol Chem* 2005;280:17005–12.

21. Ringwood L, Li L. The involvement of the interleukin-1 receptor-associated kinases (IRAKs) in cellular signaling networks controlling inflammation. *Cytokine*. 2008 Apr;42(1):1-7.

22. Su J, Xie Q, Wilson I, Li L. Differential regulation and role of interleukin-1 receptor associated kinase-M in innate immunity signaling. *Cell Signal*. 2007 Jul;19(7):1596-601

23. Su J, Zhang T, Tyson J, Li L. The Interleukin-1 Receptor-Associated Kinase M Selectively Inhibits the Alternative, Instead of the Classical NFkappaB Pathway. *J Innate Immun*. 2009 Jan 1;1(2):164-174

24. Li H, Cuartas E, Cui W, Choi Y, Crawford TD, Ke HZ, Kobayashi KS, Flavell RA, Vignery A. IL-1 receptor-associated kinase M is a central regulator of osteoclast differentiation and activation. *J Exp Med*. 2005 Apr 4;201(7):1169-77.

25. Nakayama K, Okugawa S, Yanagimoto S, Kitazawa T, Tsukada K, Kawada M, Kimura S, Hirai K, Takagaki Y, Ota Y Involvement of IRAK-M in peptidoglycan-induced tolerance in macrophages. *J Biol Chem*. 2004 Feb 20;279(8):6629-34.

26. Escoll P, del Fresno C, García L, Vallés G, Lendínez MJ, Arnalich F, López-Collazo E. Rapid up-regulation of IRAK-M expression following a second endotoxin challenge in human monocytes and in monocytes isolated from septic patients. *Biochem Biophys Res Commun*. 2003 Nov 14;311(2):465-72.

27. del Fresno C, Gómez-García L, Caveda L, Escoll P, Arnalich F, Zamora R, López-Collazo E. Nitric oxide activates the expression of IRAK-M via the release of TNF-alpha in human monocytes. *Nitric Oxide*. 2004 Jun;10(4):213-20.

28. del Fresno C, Otero K, Gómez-García L, González-León MC, Soler-Ranger L, Fuentes-Prior P, Escoll P, Baos R, Caveda L, García F, Arnalich F, López-Collazo E. Tumor cells deactivate human monocytes by up-regulating IL-1 receptor associated kinase-M expression via CD44 and TLR4. *J Immunol*. 2005 Mar 1;174(5):3032-40.

29. Pathak SK, Basu S, Bhattacharyya A, Pathak S, Kundu M, Basu J. Mycobacterium tuberculosis lipoarabinomannan-mediated IRAK-M induction negatively regulates Toll-like receptor-dependent interleukin-12 p40 production in macrophages. *J Biol Chem*. 2005 Dec 30;280(52):42794-800

30. Deng JC, Cheng G, Newstead MW, Zeng X, Kobayashi K, Flavell RA, Standiford TJ. Sepsis-induced suppression of lung innate immunity is mediated by IRAK-M. *J Clin Invest*. 2006 Sep;116(9):2532-42.

31. Mages J, Dietrich H, Lang R. A genome-wide analysis of LPS tolerance in macrophages. *Immunobiology*. 2007;212(9-10):723-37

32. Gribar SC, Sodhi CP, Richardson WM, Anand RJ, Gittes GK, Branca MF, Jakub A, Shi XH, Shah S, Ozolek JA, Hackam DJ Reciprocal expression and signaling of TLR4 and TLR9 in the pathogenesis and treatment of necrotizing enterocolitis. *J Immunol*. 2009 Jan 1;182(1):636-46.

33. Hayashi T, Gray CS, Chan M, Tawatao RI, Ronacher L, McGargill MA, Datta SK, Carson DA, Corr M. Prevention of autoimmune disease by induction of tolerance to Toll-like receptor 7. *Proc Natl Acad Sci U S A*. 2009 Feb 24;106(8):2764-9

34. Hassan F, Islam S, Tumurkhuu G, Dagvadorj J, Naiki Y, Komatsu T, Koide N, Yoshida T, Yokochi T. Involvement of interleukin-1 receptor-associated kinase (IRAK)-M in toll-like receptor (TLR) 7-mediated tolerance in RAW 264.7 macrophage-like cells. *Cell Immunol*. 2009;256(1-2):99-103.

35. Cabanski M, Wilhelm J, Zaslona Z, Steinmüller M, Fink L, Seeger W, Lohmeyer J. Genome-wide transcriptional profiling of mononuclear phagocytes recruited to mouse lungs in response to alveolar challenge with the TLR2 agonist Pam3CSK4. *Am J Physiol Lung Cell Mol Physiol*. 2009 Oct;297(4):L608-18

36. Zacharioudaki V, Androulidaki A, Arranz A, Vrentzos G, Margioris AN, Tsatsanis C Adiponectin promotes endotoxin tolerance in macrophages by inducing IRAK-M expression. *J Immunol*. 2009 May 15;182(10):6444-51

37. Bin LH, Xu LG, Shu HB. TIRP, a novel Toll/interleukin-1 receptor (TIR) domain-containing adapter protein involved in TIR signaling. *J Biol Chem*. 2003 Jul 4;278(27):24526-32.

38. Nguyen T, De Nardo D, Masendycz P, Hamilton JA, Scholz GM. Regulation of IRAK-1 activation by its C-terminal domain. *Cell Signal*. 2009 May;21(5):719-26..

39. van 't Veer C, van den Pangaart PS, van Zoelen MA, de Kruijff M, Birjmohun RS, Stroes ES, de Vos AF, van der Poll T. Induction of IRAK-M is associated with lipopolysaccharide tolerance in a human endotoxemia model. *J Immunol*. 2007 Nov 15;179(10):7110-20.

40. Gavrillin MA, Knatz NL, Duncan MD, Fernandez SA, Wewers MD. *Pediatr Res*. 2007 Nov;62(5):597-603.

41. del Fresno C, Soler-Rangel L, Soares-Schanoski A, Gómez-Piña V, González-León MC, Gómez-García L, Mendoza-Barberá E, Rodríguez-Rojas A, García F, Fuentes-Prior P, Arnalich F, López-Collazo Inflammatory responses associated with acute coronary syndrome up-regulate IRAK-M and induce endotoxin tolerance in circulating monocytes. *E.J Endotoxin Res.* 2007;13(1):39-52.
42. Wiersinga WJ, van't Veer C, van den Pangaart PS, Dondorp AM, Day NP, Peacock SJ, van der Poll T Immunosuppression associated with interleukin-1R-associated-kinase-M upregulation predicts mortality in Gram-negative sepsis (melioidosis). *Crit Care Med.* 2009 Feb;37(2):569-76.
43. IRAK-M is involved in the pathogenesis of early-onset persistent asthma. Balaci L, Spada MC, Olla N, Sole G, Loddo L, Anedda F, Naitza S, Zuncheddu MA, Maschio A, Altea D, Uda M, Pilia S, Sanna S, Masala M, Crisponi L, Fattori M, Devoto M, Doratiotto S, Rassu S, Mereu S, Giua E, Cadeddu NG, Atzeni R, Pelosi U, Corrias A, Perra R, Torrazza PL, Pirina P, Ginesu F, Marcias S, Schintu MG, Del Giacco GS, Manconi PE, Malerba G, Bisognin A, Trabetti E, Boner A, Pescollderung L, Pignatti PF, Schlessinger D, Cao A, Pilia G. *Am J Hum Genet.* 2007 Jun;80(6):1103-14.
44. Berclaz PY, Carey B, Fillipi MD, Wernke-Dollries K, Geraci N, Cush S, Richardson T, Kitzmiller J, O'connor M, Hermoyian C, Korfhagen T, Whitsett JA, Trapnell BC. GM-CSF regulates a PU.1-dependent transcriptional program determining the pulmonary response to LPS. *Am J Respir Cell Mol Biol.* 2007 Jan;36(1):114-21.
45. Soares-Schanoski A, Gómez-Piña V, del Fresno C, Rodríguez-Rojas A, García F, Glaría A, Sánchez M, Vallejo-Cremades MT, Baos R, Fuentes-Prior P, Arnalich F, López-Collazo E. 6-Methylprednisolone down-regulates IRAK-M in human and murine osteoclasts and boosts bone-resorbing activity: a putative mechanism for corticoid-induced osteoporosis. *J Leukoc Biol.* 2007 Sep;82(3):700-9.
46. Sly LM, Rauh MJ, Kalesnikoff J, Song CH, Krystal G. LPS-induced upregulation of SHIP is essential for endotoxin tolerance. *Immunity.* 2004 Aug;21(2):227-39.
47. Inhibition of TLR activation and up-regulation of IL-1R-associated kinase-M expression by exogenous gangliosides. Shen W, Stone K, Jales A, Leitenberg D, Ladisch S. *J Immunol.* 2008 Apr 1;180(7):4425-32
48. Hornef, M. W., B. H. Normark, A. Vandewalle, and S. Normark. 2003. Intracellular recognition of lipopolysaccharide by Toll-like receptor 4 in intestinal epithelial cells. *J. Exp. Med.* 198: 1225–1235.
49. Gribar SC, Sodhi CP, Richardson WM, Anand RJ, Gittes GK, Branca MF, Jakub A, Shi XH, Shah S, Ozolek JA, Hackam DJ. Reciprocal expression and signaling of TLR4 and TLR9 in the pathogenesis and treatment of necrotizing enterocolitis. *J Immunol.* 2009 Jan 1;182(1):636-46.
50. Xie Q, Gan L, Wang J, Wilson I, Li L. Loss of the innate immunity negative regulator IRAK-M leads to enhanced host immune defense against tumor growth. *Mol Immunol.* 2007 Jul;44(14):3453-61.
51. Lin X, Cunningham ET Jr, Mu Y, Gelezianas R, Greene WC The proto-oncogene Cot kinase participates in CD3/CD28 induction of NF-kappaB acting through the NF-kappaB-inducing kinase and IkkappaB kinases. *Immunity.* 1999 Feb;10(2):271-80.
52. Das S, Cho J, Lambert J, Kelliher MA, Eliopoulos AG, Du K, Tsichlis PN. Tpl2/cot signals activate ERK, JNK, and NF-kappaB in a cell-type and stimulus-specific manner. *J Biol Chem.* 2005 Jun 24;280(25):23748-57.
53. Ozes, O. N., L. D. Mayo, J. A. Gustin, S. R. Pfeffer, L. M. Pfeffer, and D. B. Donner. 1999. NF- κ B activation by tumor necrosis factor requires the Akt serine-threonine kinase. *Nature* 401: 82–85.
54. Rieske, P., and J. M. Pongubala. 2001. AKT induces transcriptional activity of PU.1 through phosphorylation-mediated modifications within its transactivation domain. *J. Biol. Chem.* 276: 8460–8468.
55. Piwien-Pilipuk G, Van Mater D, Ross SE, MacDougald OA, Schwartz J. Growth hormone regulates phosphorylation and function of CCAAT/enhancer-binding protein beta by modulating Akt and glycogen synthase kinase-3. *J Biol Chem.* 2001 Jun 1;276(22):19664-71.
56. Tanaka, T., M. Kurokawa, K. Ueki, K. Tanaka, Y. Imai, K. Mitani, K. Okazaki, N. Sagata, Y. Yazaki, Y. Shibata, T. Kadowaki, and H. Hirai. 1996. The extracellular signal-regulated kinase pathway phosphorylates AML1, an acute myeloid leukemia gene product, and potentially regulates its transactivation ability. *Mol. Cell. Biol.* 16:3967–3979.
57. Petrovick MS, Hiebert SW, Friedman AD, Hetherington CJ, Tenen DG, Zhang DE. Multiple functional domains of AML1: PU.1 and C/EBPalpha synergize with different regions of AML1. *Mol Cell Biol.* 1998 Jul;18(7):3915-25.
58. Pan H, Ding E, Hu M, Lagoo AS, Datto MB, Lagoo-Deenadayalan SA SMAD4 is required for development of maximal endotoxin tolerance. *J Immunol.* 2010 May 15;184(10):5502-9.

59. C. Gregori, A. Kahn* and A.-L. Pichard Competition between transcription factors HNF1 and HNF3, and alternative cell-specific activation by DBP and C/EBP contribute to the regulation of the liver-specific aldolase B promoter *Nucleic Acids Research*, 1993, Vol. 21, No. 4 897-903
60. Park PH, McMullen MR, Huang H, Thakur V, Nagy LE Short-term treatment of RAW264.7 macrophages with adiponectin increases tumor necrosis factor-alpha (TNF-alpha) expression via ERK1/2 activation and Egr-1 expression: role of TNF-alpha in adiponectin-stimulated interleukin-10 production. *J Biol Chem*. 2007 Jul 27;282(30):21695-703. Epub 2007 May 30.
61. Apostolou E, Thanos D Virus Infection Induces NF-kappaB-dependent interchromosomal associations mediating monoallelic IFN-beta gene expression. *Cell*. 2008 Jul 11;134(1):85-96
62. Yu H, Pardoll D, Jove R. STATs in cancer inflammation and immunity: a leading role for STAT3. *Nat Rev Cancer*. 2009 Nov;9(11):798-809
63. Sweet MJ, Hume DA Endotoxin signal transduction in macrophages. *J Leukoc Biol*. 1996 Jul;60(1):8-26.
64. Cappello C, Zwergal A, Kanclerski S, Haas SC, Kandemir JD, Huber R, Page S, Brand K. C/EBPbeta enhances NF-kappaB-associated signalling by reducing the level of IkappaB-alpha. *Cell Signal*. 2009 Dec;21(12):1918-24
65. Kramer F, Torzewski J, Kamenz J, Veit K, Hombach V, Dedio J, Ivashchenko Y. Interleukin-1beta stimulates acute phase response and C-reactive protein synthesis by inducing an NFkappaB- and C/EBPbeta-dependent autocrine interleukin-6 loop. *Mol Immunol*. 2008 May;45(9):2678-89
66. Matsuo S, Yamazaki S, Takeshige K, Muta T Crucial roles of binding sites for NF-kappaB and C/EBPs in IkappaB-zeta-mediated transcriptional activation. *Biochem J*. 2007 Aug 1;405(3):605-15.
67. Fukao, T., and Koyasu, S. (2003). PI3K and negative regulation of TLR signaling. *Trends Immunol* 24, 358-363
68. Li Y, Bevilacqua E, Chiribau CB, Majumder M, Wang C, Croniger CM, Snider MD, Johnson PF, Hatzoglou M. Differential control of the CCAAT/enhancer-binding protein beta (C/EBPbeta) products liver-enriched transcriptional activating protein (LAP) and liver-enriched transcriptional inhibitory protein (LIP) and the regulation of gene expression during the response to endoplasmic reticulum stress. *J Biol Chem*. 2008 Aug 15;283(33):22443-56.
69. Sica, A., and V. Bronte. 2007. Altered macrophage differentiation and immune dysfunction in tumor development. *J. Clin. Invest.* 117: 1155–1166.
70. Ilaria Marigo, Erika Bosio, Samantha Solito, Circe Mesa, Audry Fernandez, Luigi Dolcetti, Stefano Ugel, Nada Sonda, Silvio Biccato, Erika Falisi, Fiorella Calabrese, Giuseppe Basso, Paola Zanovello, Emanuele Cozzi, Susanna Mandruzzato and Vincenzo Bronte, Tumor induced tolerance and immune suppression depend on the C/EBP transcription factor. *Immunity* 32, 790–802, June 25, 2010